

PERFORMANCE OF CONTAINMENT VESSEL UNDER SEVERE ACCIDENT CONDITIONS

SPE analysis meeting #2
April 13-14, 2011, Washington DC

SUMMARY

- Model 1** : **Sensitivity analyses & findings**
- ⋮
- Model 2** : **Methodology & difficulties**



Juan-José GAYETE

Charles GHAVAMIAN

Thibault MARTIN

Mahsa MOZAYAN KHARAZI

Sylvie MICHEL-PONNELLE

Etienne GALLITRE

Model 1

SUMMARY

Sensitivity analyses

- Mesh discretisation
- Mesh element type
- Concrete constitutive law
- Concrete constitutive law parameters
- Tendon / Duct interaction

Modelling technique

Concrete

Solid element

Linear and quadratic configurations

Mesh size: described in another section

steel reinforcement

Grid elements

Shell element with uniaxial behaviour

Linear

Rebar / concrete interface: perfectly bonded

Placed on inner and outer surfaces of concrete mesh

Liner

Shell elements

Thickness 1.6mm

Liner perfectly bonded with concrete

Hoop tendons

Truss elements

Tendon / concrete interface: 3 configurations

1- Grouted ducts: perfectly bonded

2- Slippery ducts (perfectly bonded in Z and R direction, free along tendon direction)

3- Ungrouted ducts (perfectly bonded in Z and R direction, friction along tendon direction)

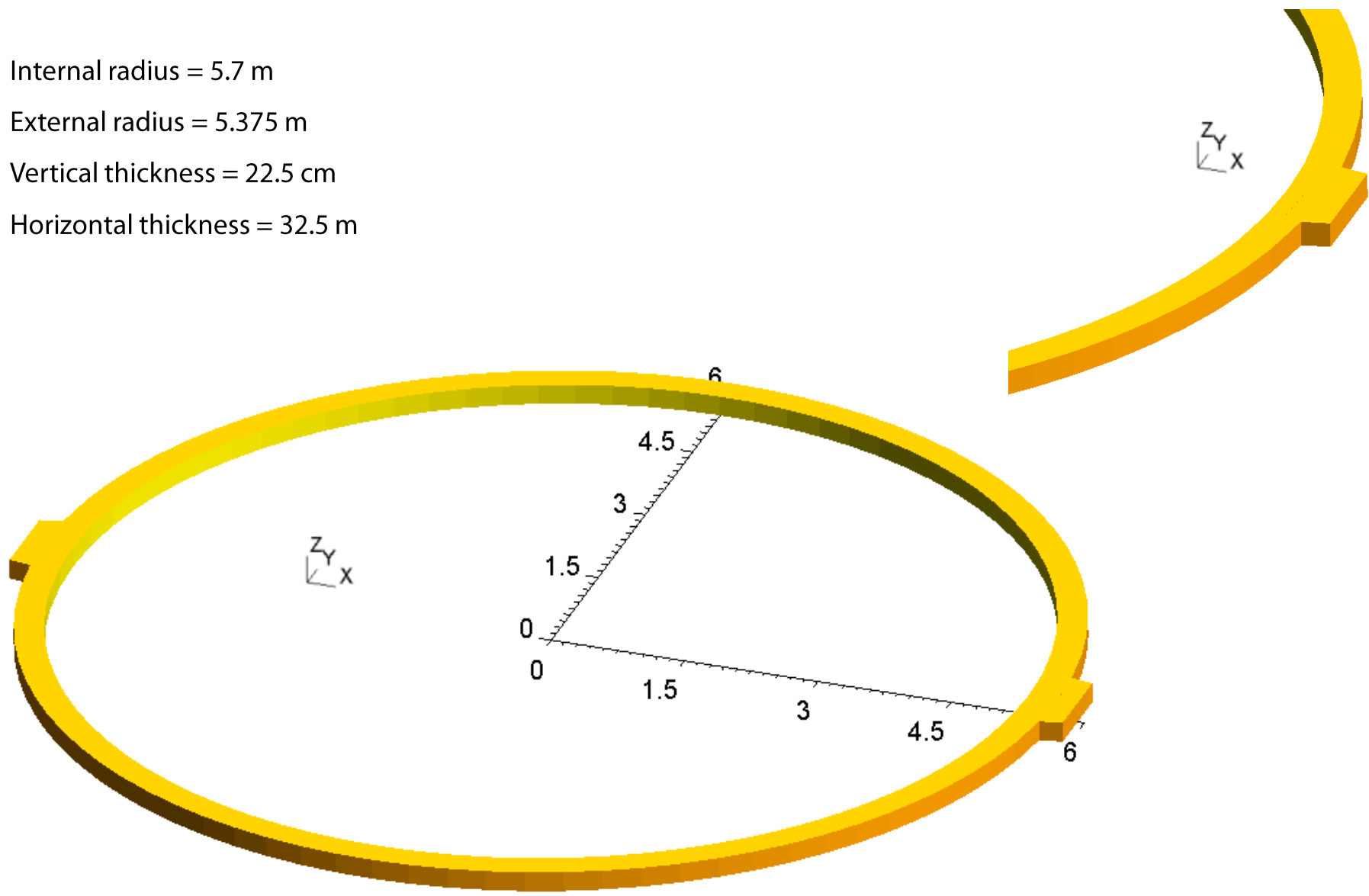
Model geometry

Internal radius = 5.7 m

External radius = 5.375 m

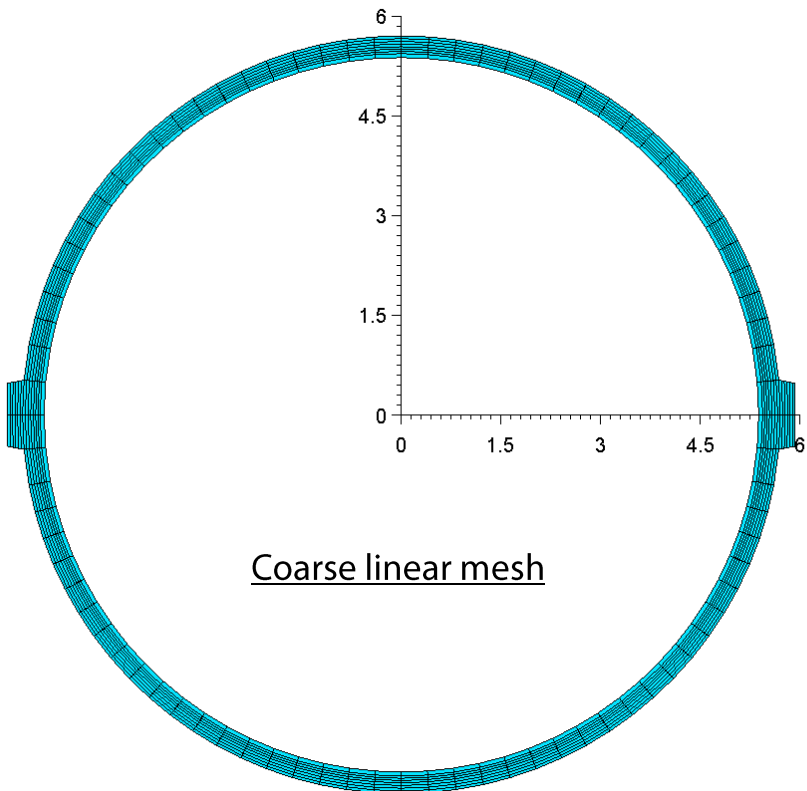
Vertical thickness = 22.5 cm

Horizontal thickness = 32.5 m

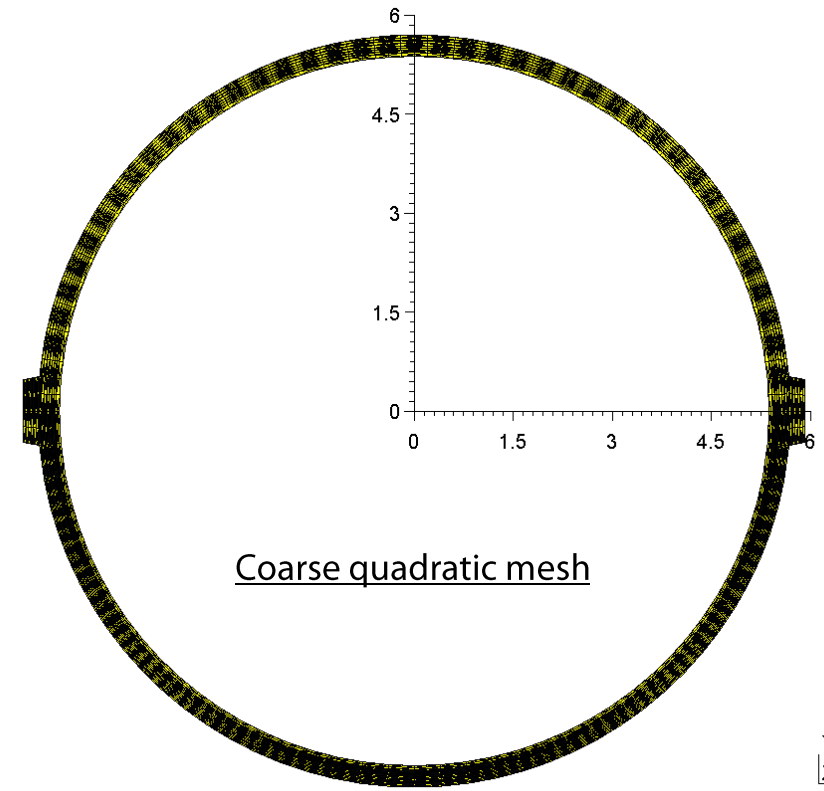


Mesh discretisation

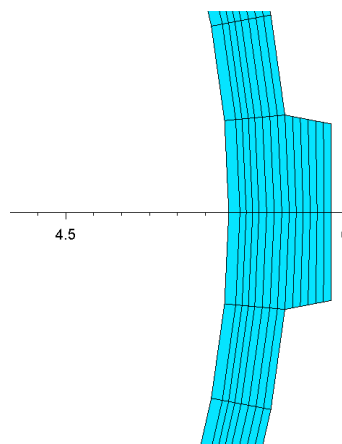
3 situations



Coarse linear mesh

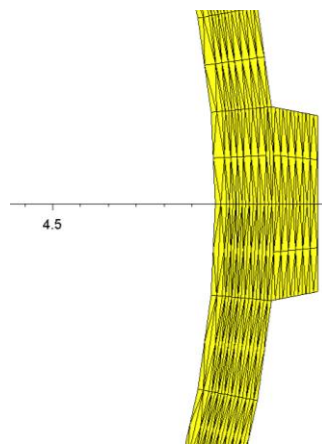


Coarse quadratic mesh

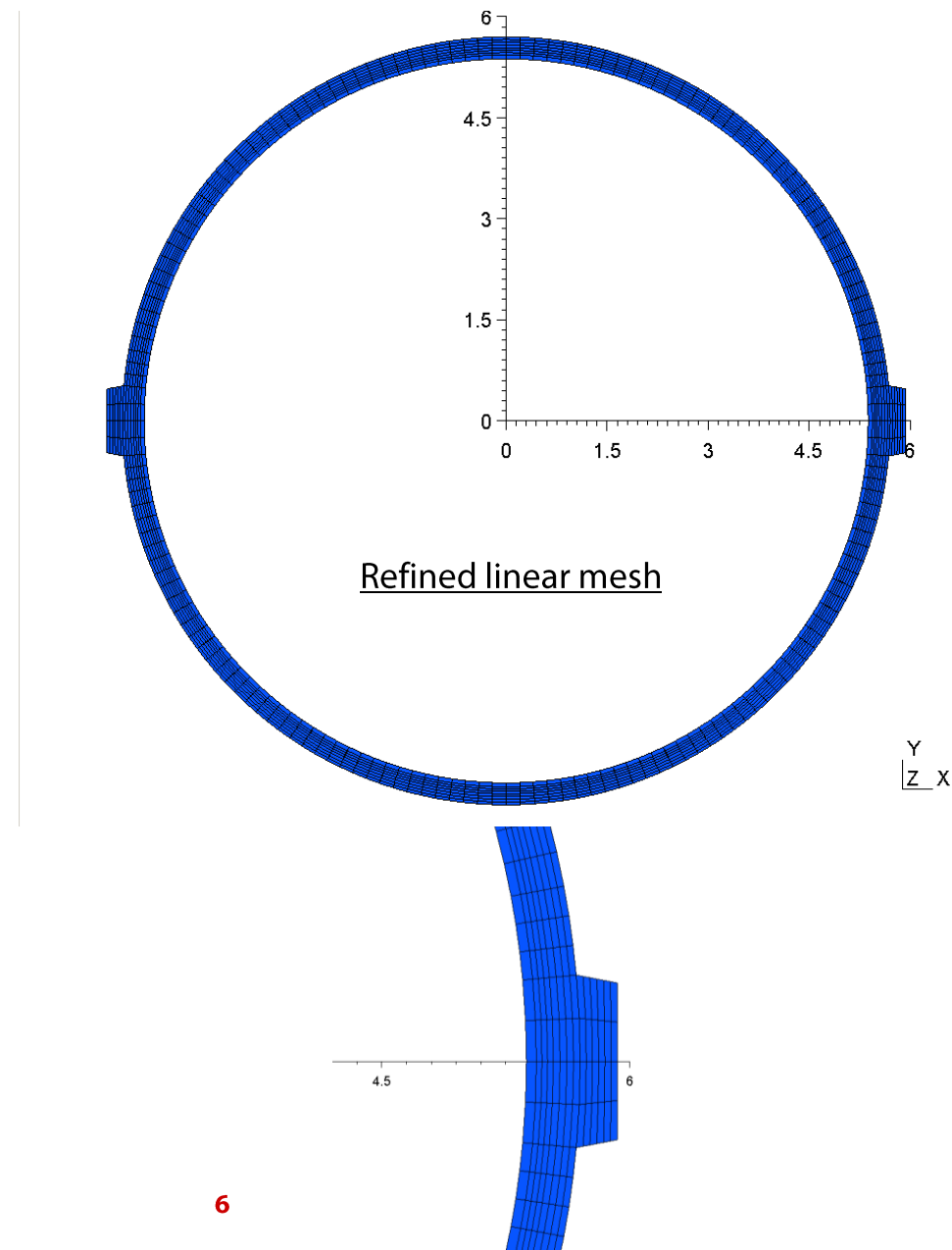


A1

5



Mesh discretisation

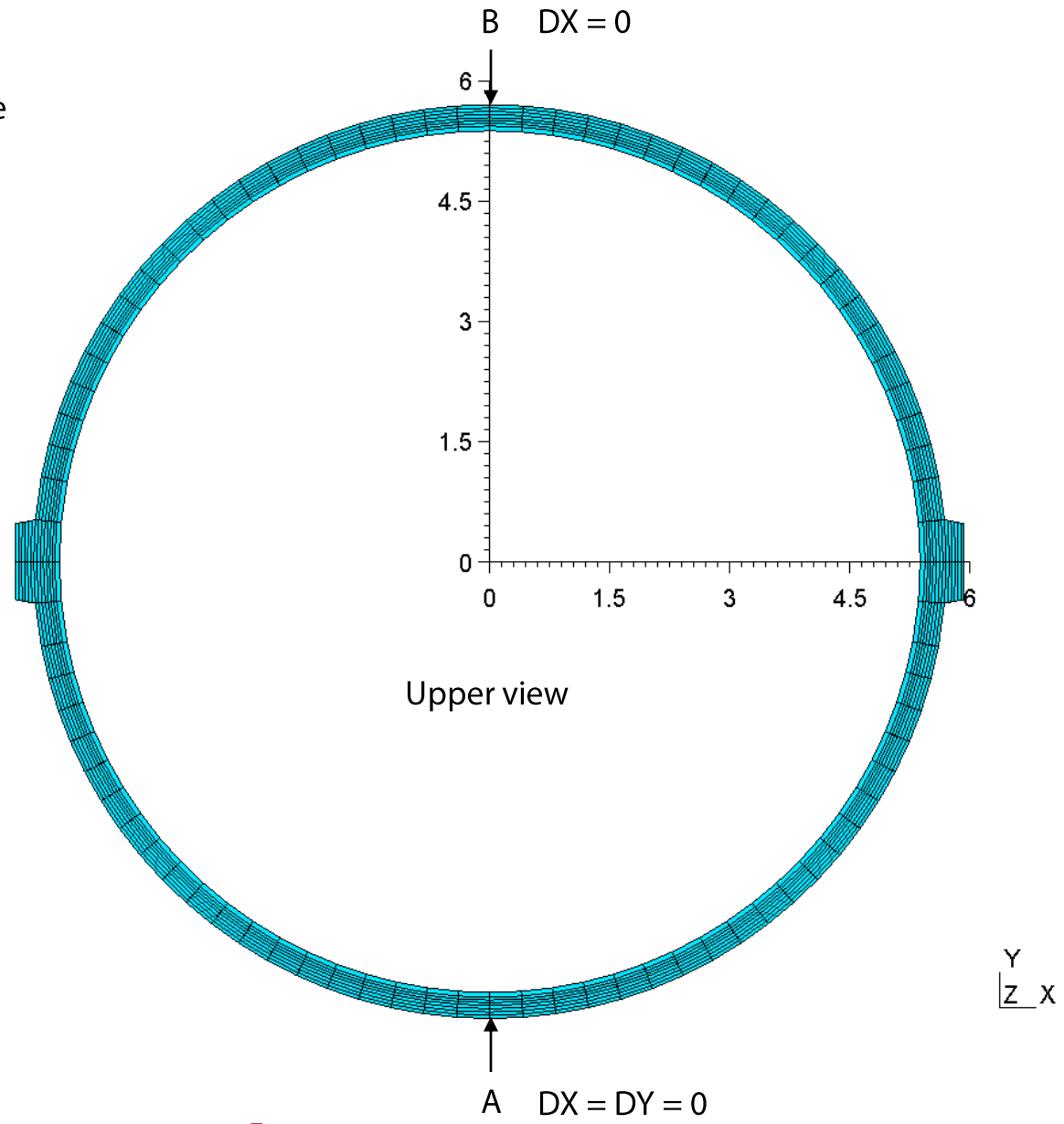


Boundary conditions

Upper face: Z DOF follow the same value

Lower face: DZ=0

See figure for the others



Concrete constitutive model

Known as "Mazars"

Features :

- Based on damage mechanics
- Unilateral behaviour (tension / compression distinction)
- Isotropic damage effect (single scalar damage index D)
- No crack reclosure (not suitable for cyclic loading)

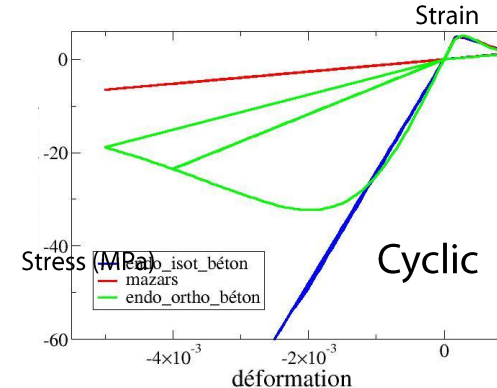
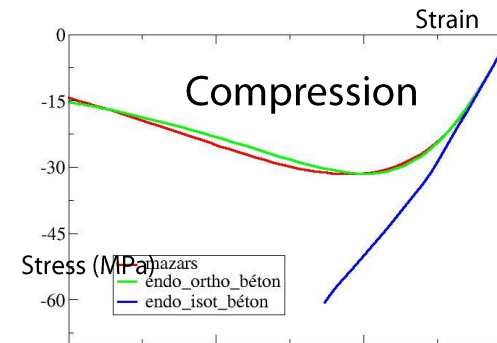
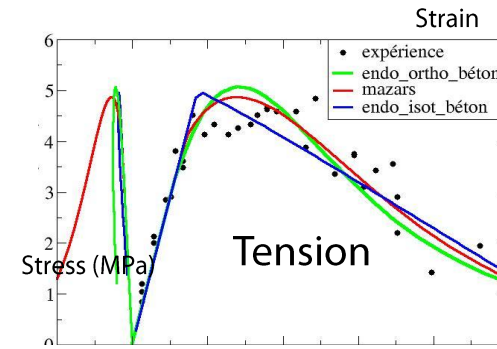
$$\sigma_{ij} = (1 - D) C_{ijkl} \varepsilon_{kl}$$

$$D = \alpha_t D_t + \alpha_c D_c$$

$$\alpha_{t,c} = \left(\sum_{i=1}^3 \frac{<\varepsilon_i^{t,c}> <\varepsilon_i>_+}{\varepsilon_{eq}^2} \right)^\beta \quad D_{t,c} = 1 - \frac{\varepsilon_{eq,0}(1 - A_{t,c})}{\varepsilon_{eq}} - \frac{A_{t,c}}{\exp[B_{t,c}(\varepsilon_{eq} - \varepsilon_{eq,0})]}$$

$$\varepsilon_{eq} = \sqrt{\sum_{i=1}^3 (<\varepsilon_i>_+)^2}$$

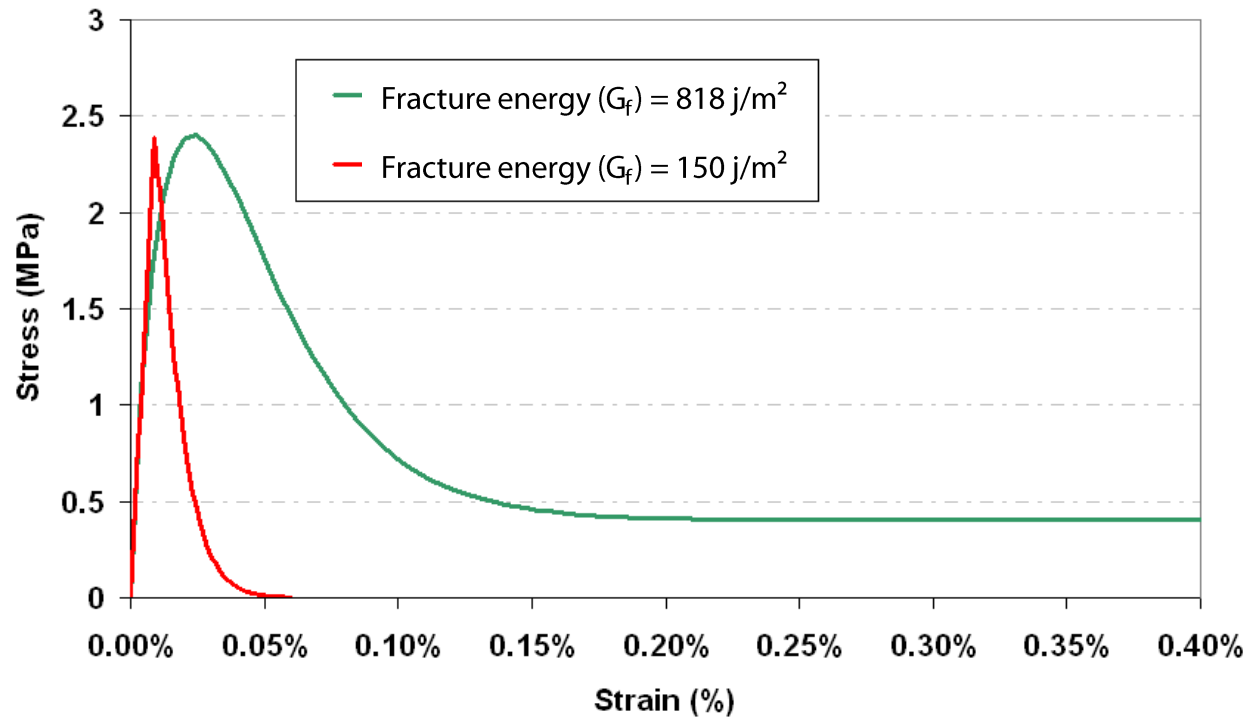
Mazars : red curves



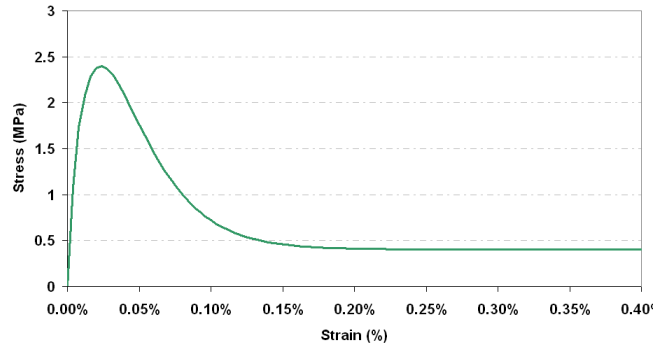
Concrete constitutive model

Material parameter set	M818	M150
Fracture energy (G_f)	818 j/m ²	150 j/m ²
Mesh size	43 cm	43 cm
Young's Modulus (E)	26 900 MPa	26 900 MPa
Poisson's ratio (v)	0.21	0.21
Density (ρ)	2 176 kg/m ³	2 176 kg/m ³
Tensile Strength (f_t)	2.4 MPa	2.4 MPa
Strain	0.024%	0.009%
Compressive Strength (f_c)	61 MPa	62 MPa
Strain	0.54%	0.54%

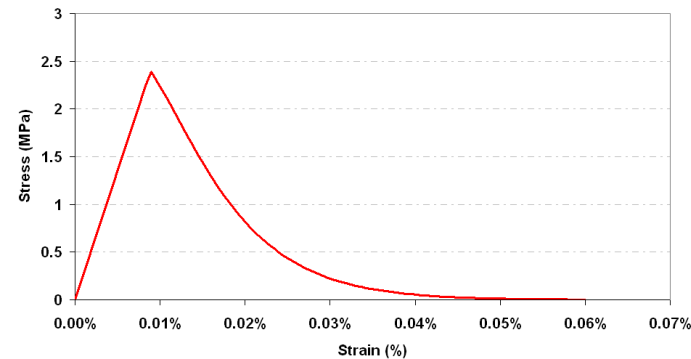
Concrete constitutive model



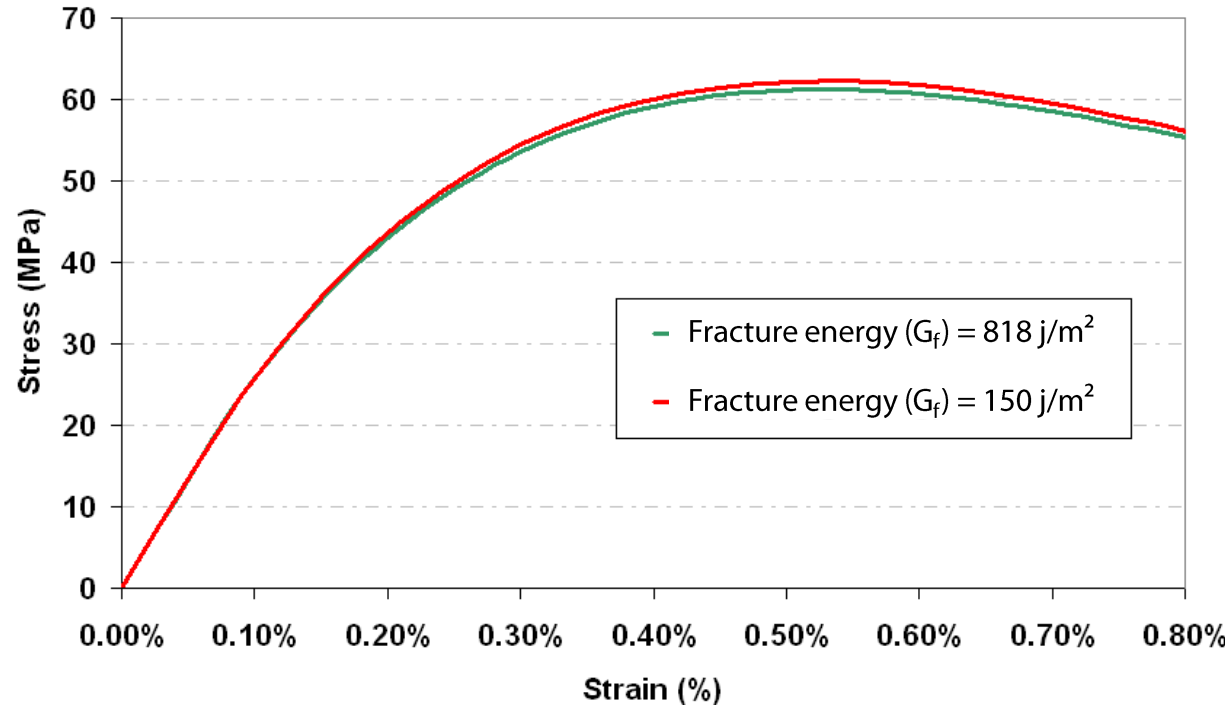
Tensile behaviour (Cracking Energy = 818 N/m)



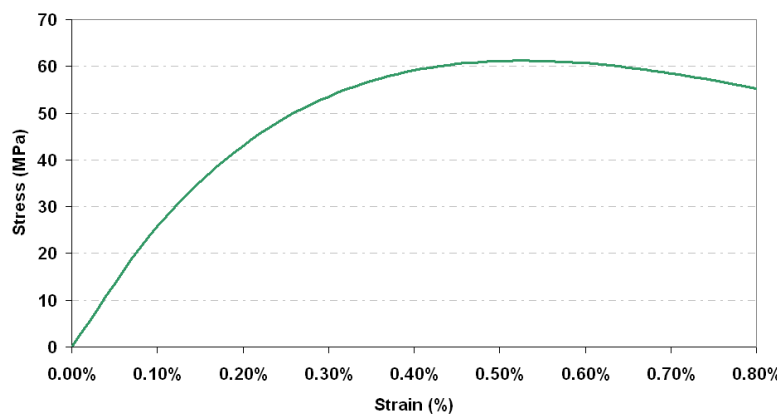
Tensile behaviour (Cracking Energy = 150 N/m)



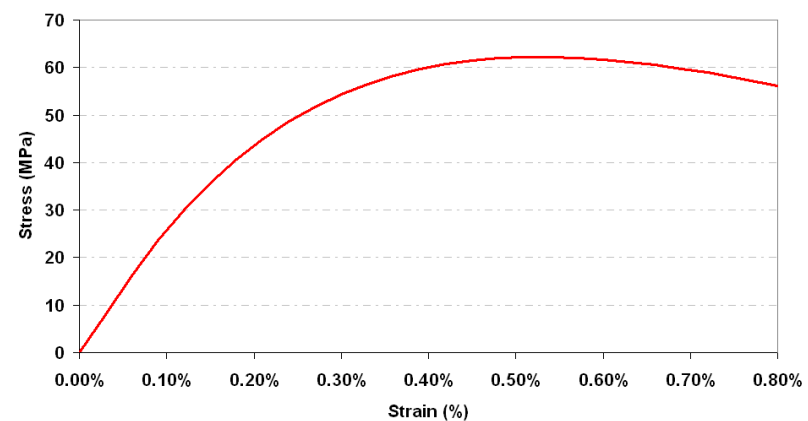
Concrete constitutive model



Compressive behaviour (Cracking Energy = 818 N/m)



Compressive behaviour (Cracking Energy = 150 N/m)



Liner steel constitutive model

Elastoplastic

Parameters:

Young's Modulus (E) = 210 000 MPa

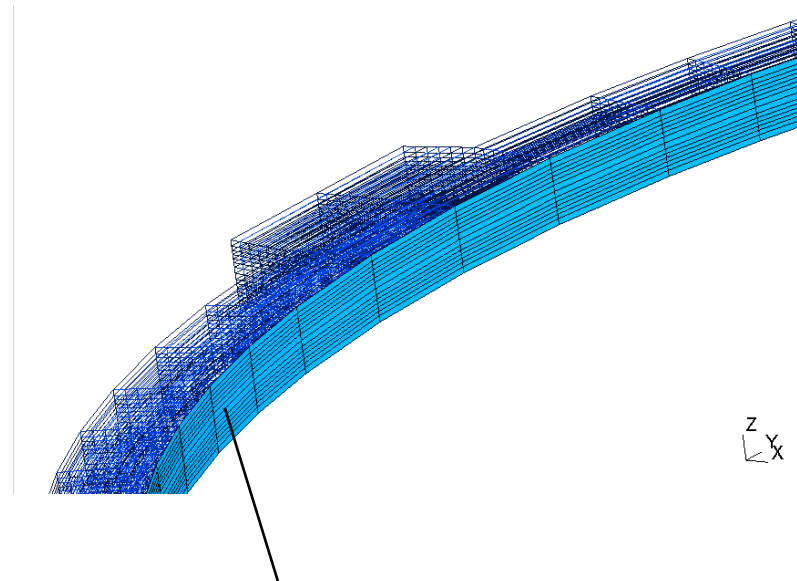
Young Modulus in plastic phase (E) = 927 MPa

Poisson's ratio (ν) = 0.3

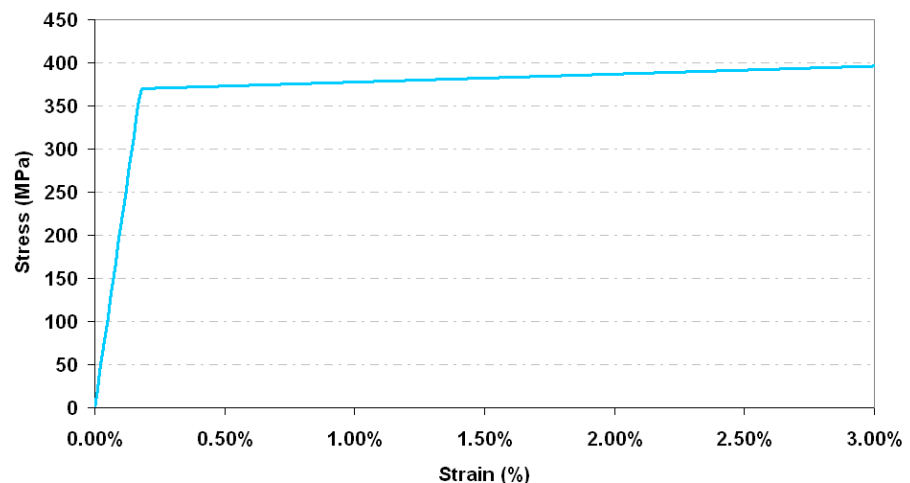
Density (ρ) = 7850 kg/m³

Yield Strength (Y_s) = 370 MPa

Density (ρ) = 7 850 kg/m³



Liner thickness = 1.6 mm



Tendon steel constitutive model

Elastoplastic

Parameters:

Young Modulus in elastic phase (E) = 191 000 MPa

Young Modulus in plastic phase (E) = 5 894 MPa

Poisson's ratio (ν) = 0.3

Density (ρ) = 7850 kg/m³

Yield Strength (Y_s) = 1 679 MPa

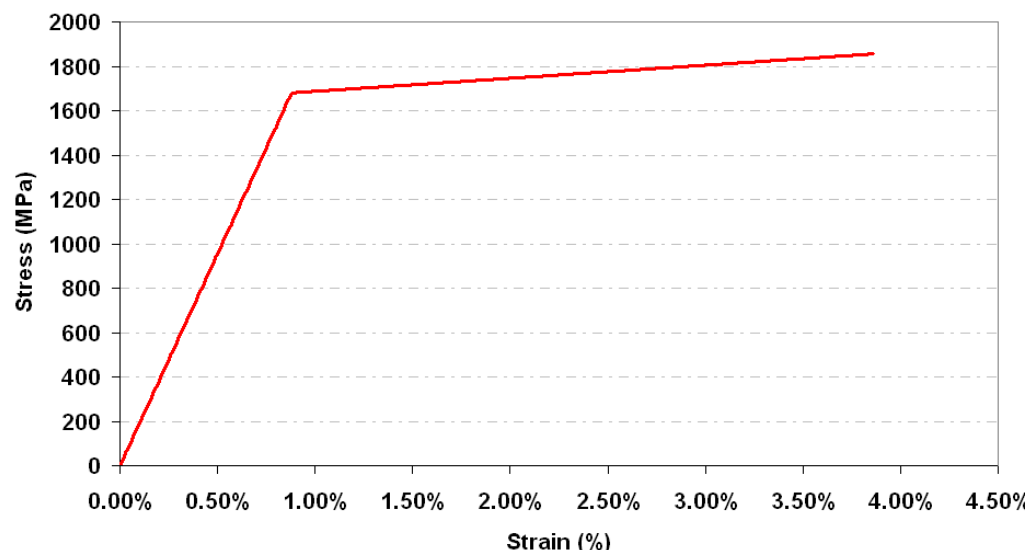
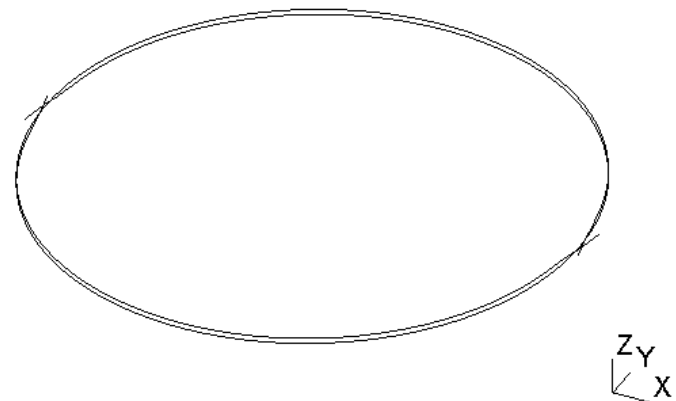
Tensile Strength (XXX) = 1 856.76 MPa

Density (ρ) = 7850 kg/m³

Setting Losses = 3.95 mm

Angular and wobble friction: $\mu = 0.21$; $\lambda = 0.001$

Tendons section = 3.393 cm² (each tendon)



Tendon steel constitutive model

Elastoplastic

Parameters:

Young Modulus in elastic phase (E) = 185 000 MPa

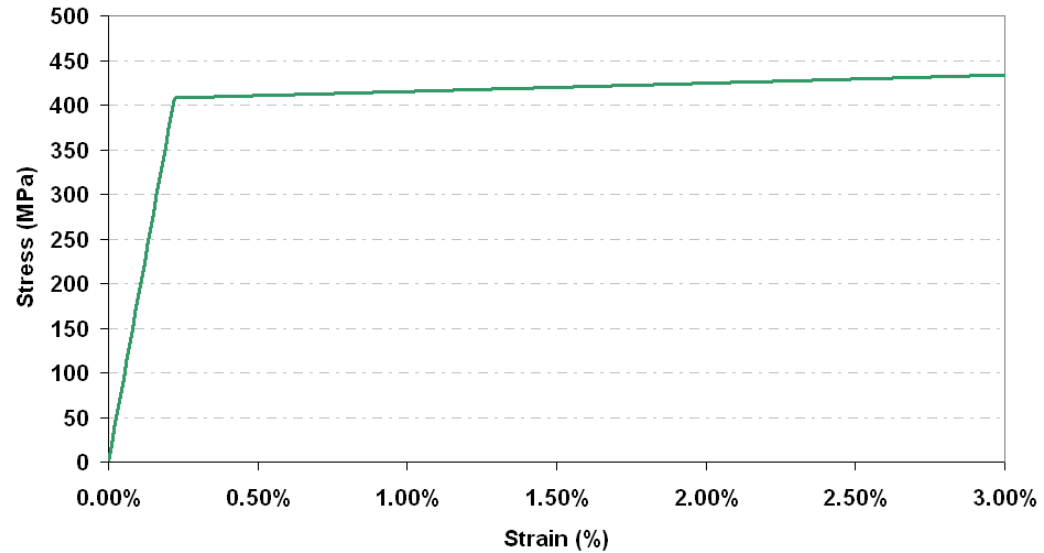
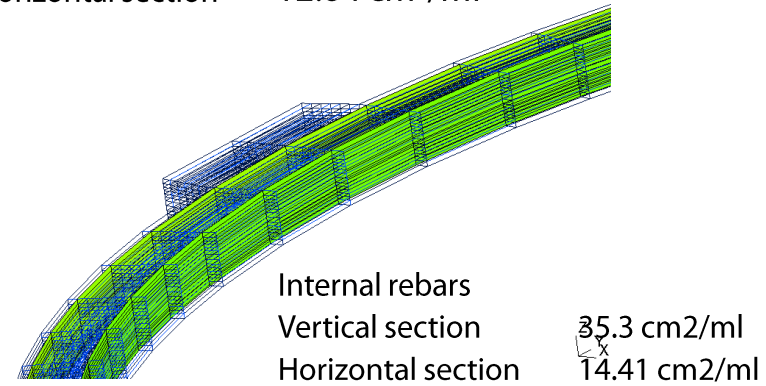
Young Modulus in plastic phase (E) = 927 MPa

Poisson's ratio (ν) = 0.3

Density (ρ) = 7 850 kg/m³

Yield Strength (Y_s) = 408 MPa

External rebars	35.3 cm ² /ml
Vertical section	12.84 cm ² /ml
Horizontal section	



Loading

Initial condition:

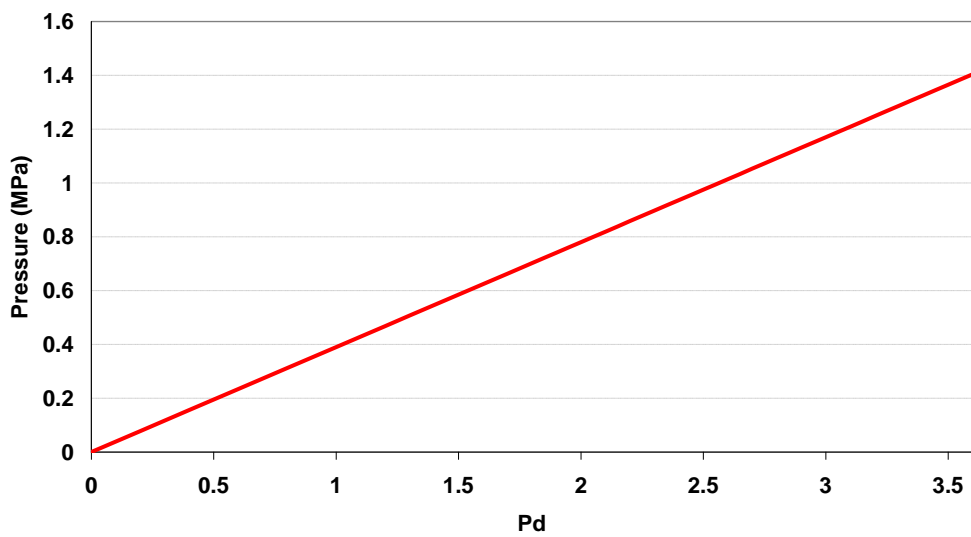
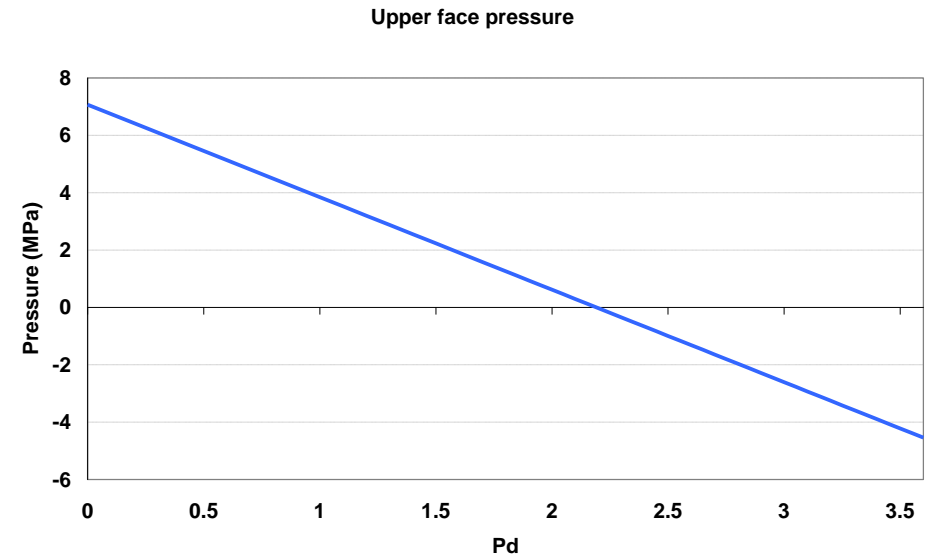
Hoop prestressing of 444 kN

Downward pressure on top surface of 7.02 MPa

followed by:

Internal pressure P

Upward pressure on top surface of $8.27 \times P$ MPa



Sensitivity analyses

Case study	Mesh	Tendon type	Concrete	Liner	Tendon	Rebar
Tendon type effect (TTE)	GROL	GD	M818	NL	NL	NL
		SD				
		NGD				
Mesh Type Effect (MTE)	GROL	GD	LE	LE	LE	LE
Cracking energy effect (CEE)	GROL	SD	M818	NL	NL	NL
			M150			

Rebar behaviour

Linear	LE
Non-linear	NL

Tendon type

Grouted duct	GD
Slippery duct	SD
Ungrounded duct	UGD

Concrete behaviour

Linear	LE
EDF_2005	MEDF
Mazars (818 j/m ² , L=0.43 m)	M818
Mazars (150 j/m ² , L=0.43 m)	M150

Meshing

Coarse - linear	GROL
Refined - linear	FINL
Coarse quadratic	GROQ

Tendon behaviour

Linear	LE
Non-linear	NL

Liner behaviour

Linear	LE
Non-linear	NL

Sensitivity analyses: tendon/duct interaction

Nonlinear analysis

With grouted duct, high strain localisation appear where concrete cracks (modelling simplification).

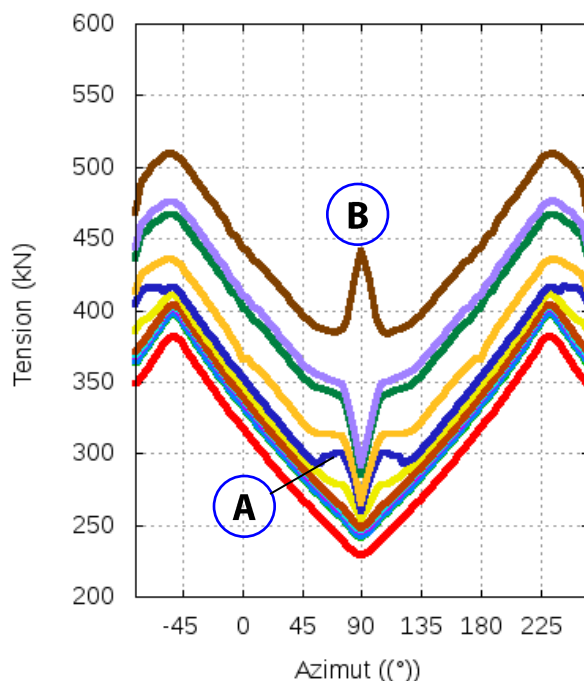
When ducts are ungrouted, localisation is less strong (representative of Sandia test).

Fully slippery ducts produce uniform tendon tension. The initial prestressing should have been lowered to encounter for losses.

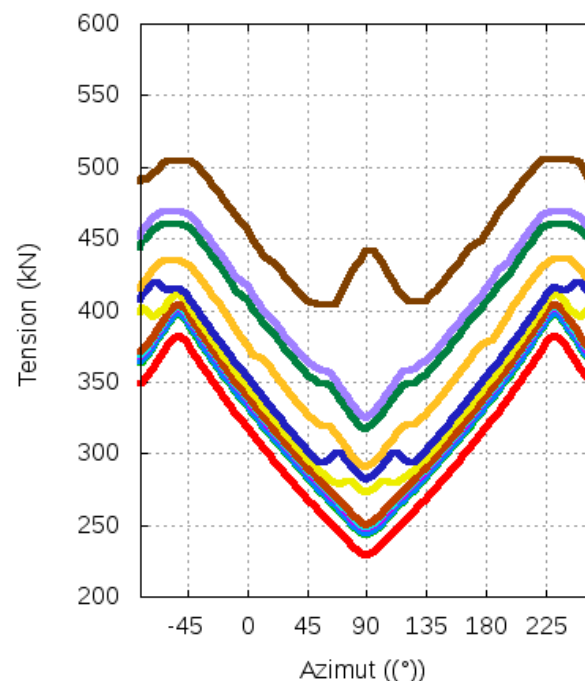
Tendon H-67 tension distribution

$P = 0.0 \text{ MPa} (0.0 \text{ Pd})$	
$P = 0.4 \text{ MPa} (1.0 \text{ Pd})$	
$P = 0.4 \text{ MPa} (1.1 \text{ Pd})$	
$P = 0.5 \text{ MPa} (1.4 \text{ Pd})$	
$P = 0.6 \text{ MPa} (1.5 \text{ Pd})$	
$P = 0.6 \text{ MPa} (1.6 \text{ Pd})$	
$P = 0.7 \text{ MPa} (1.9 \text{ Pd})$	
$P = 0.8 \text{ MPa} (2.0 \text{ Pd})$	
$P = 0.8 \text{ MPa} (2.1 \text{ Pd})$	
$P = 0.9 \text{ MPa} (2.4 \text{ Pd})$	
$P = 1.0 \text{ MPa} (2.5 \text{ Pd})$	
$P = 1.0 \text{ MPa} (2.6 \text{ Pd})$	

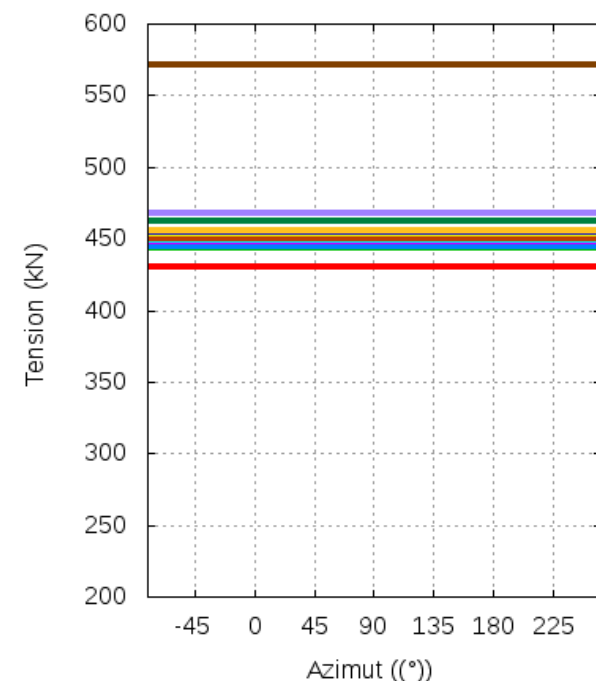
Grouted duct



Ungrounded duct



Slippery duct



Sensitivity analyses: tendon/duct interaction

Nonlinear analysis

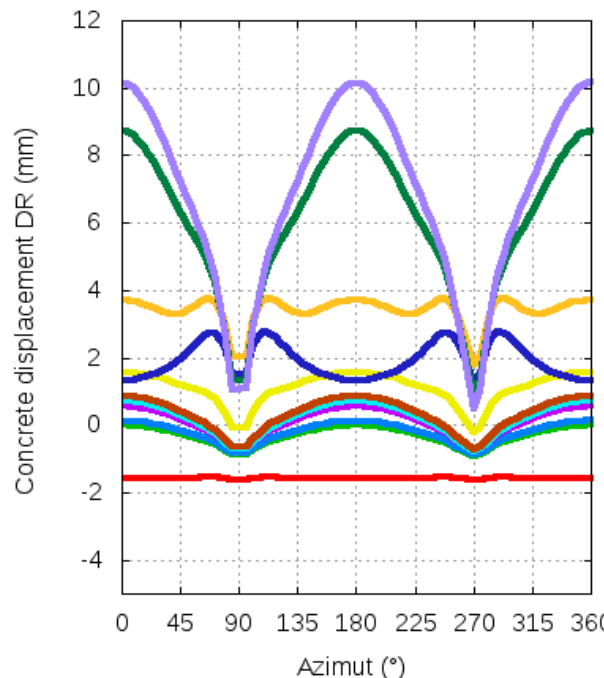
Grouted and ungrouted tendons exhibit the same radial displacements during linear elastic range of behaviour. This is also the case at high internal pressure loading with strong concrete damage. In between, results are significantly different.

For fully slippery duct, deflections are uniform, and lower, due to stronger prestressing.

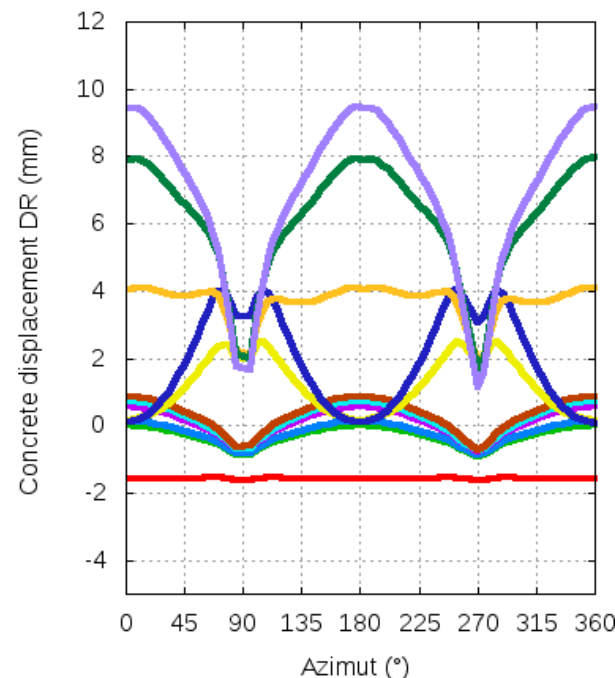
Radial displacement ($z = H/2$, external face)

$P = 0.0 \text{ MPa} (0.0 \text{ Pd})$	— red
$P = 0.4 \text{ MPa} (1.0 \text{ Pd})$	— green
$P = 0.4 \text{ MPa} (1.1 \text{ Pd})$	— blue
$P = 0.5 \text{ MPa} (1.4 \text{ Pd})$	— purple
$P = 0.6 \text{ MPa} (1.5 \text{ Pd})$	— cyan
$P = 0.6 \text{ MPa} (1.6 \text{ Pd})$	— orange
$P = 0.7 \text{ MPa} (1.9 \text{ Pd})$	— yellow
$P = 0.8 \text{ MPa} (2.0 \text{ Pd})$	— dark blue
$P = 0.8 \text{ MPa} (2.1 \text{ Pd})$	— gold
$P = 0.9 \text{ MPa} (2.4 \text{ Pd})$	— dark green
$P = 1.0 \text{ MPa} (2.5 \text{ Pd})$	— light blue

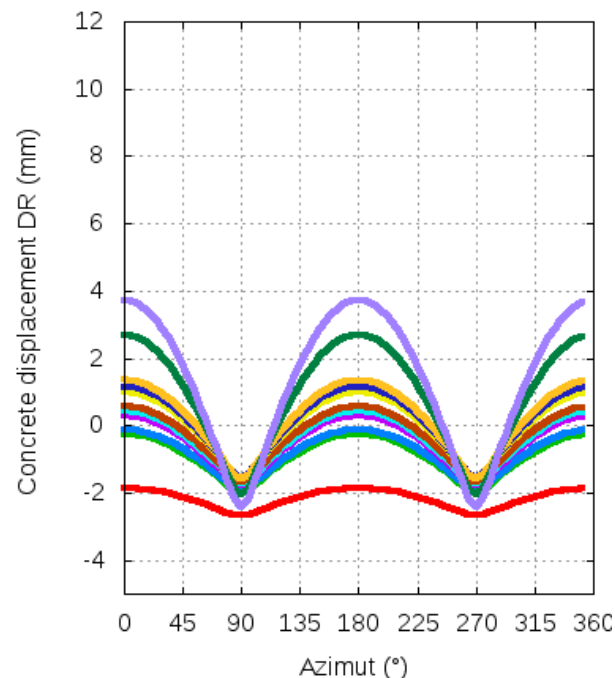
Grouted duct



Ungrounded duct



Slippery duct



Sensitivity analyses: tendon/duct interaction

Nonlinear analysis

Concrete hoop stresses are quite similar between both grouted and ungrouted tendons.

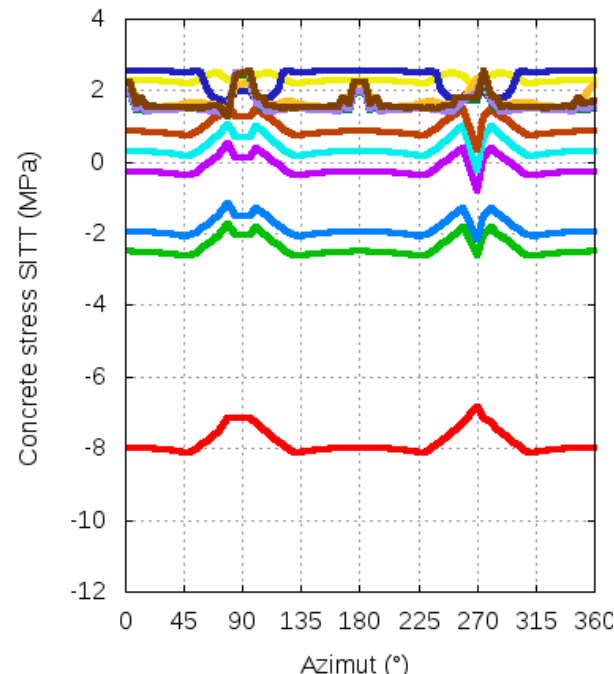
Slippery ducts lead to late cracking

Concrete hoop stress

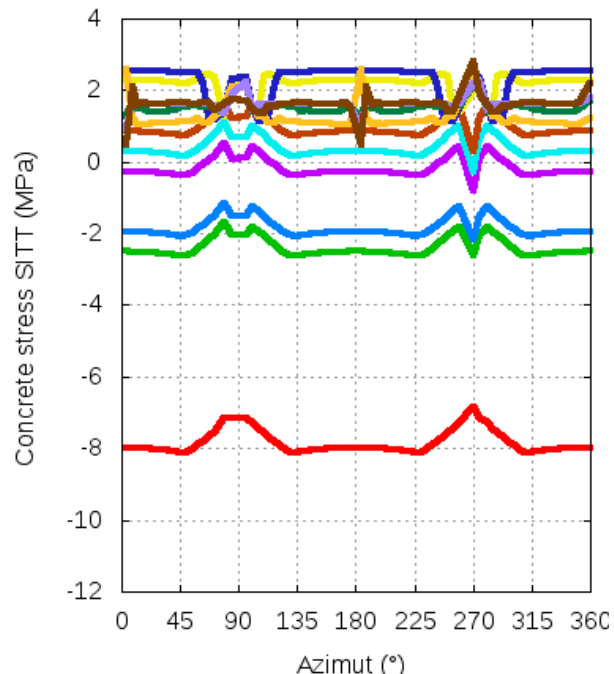
($z = H/2$, mid-section)

$P = 0.0 \text{ MPa (0.0 Pd)}$	
$P = 0.4 \text{ MPa (1.0 Pd)}$	
$P = 0.4 \text{ MPa (1.1 Pd)}$	
$P = 0.5 \text{ MPa (1.4 Pd)}$	
$P = 0.6 \text{ MPa (1.5 Pd)}$	
$P = 0.6 \text{ MPa (1.6 Pd)}$	
$P = 0.7 \text{ MPa (1.9 Pd)}$	
$P = 0.8 \text{ MPa (2.0 Pd)}$	
$P = 0.8 \text{ MPa (2.1 Pd)}$	
$P = 0.9 \text{ MPa (2.4 Pd)}$	
$P = 1.0 \text{ MPa (2.5 Pd)}$	
$P = 1.0 \text{ MPa (2.6 Pd)}$	

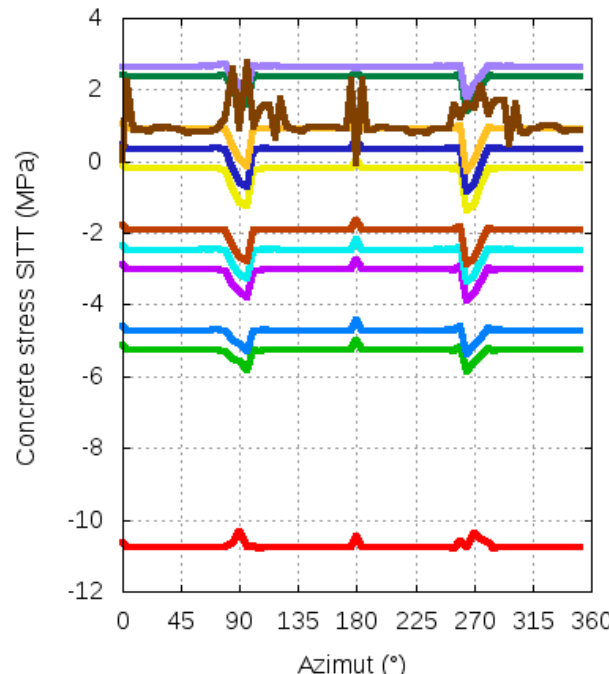
Grouted duct



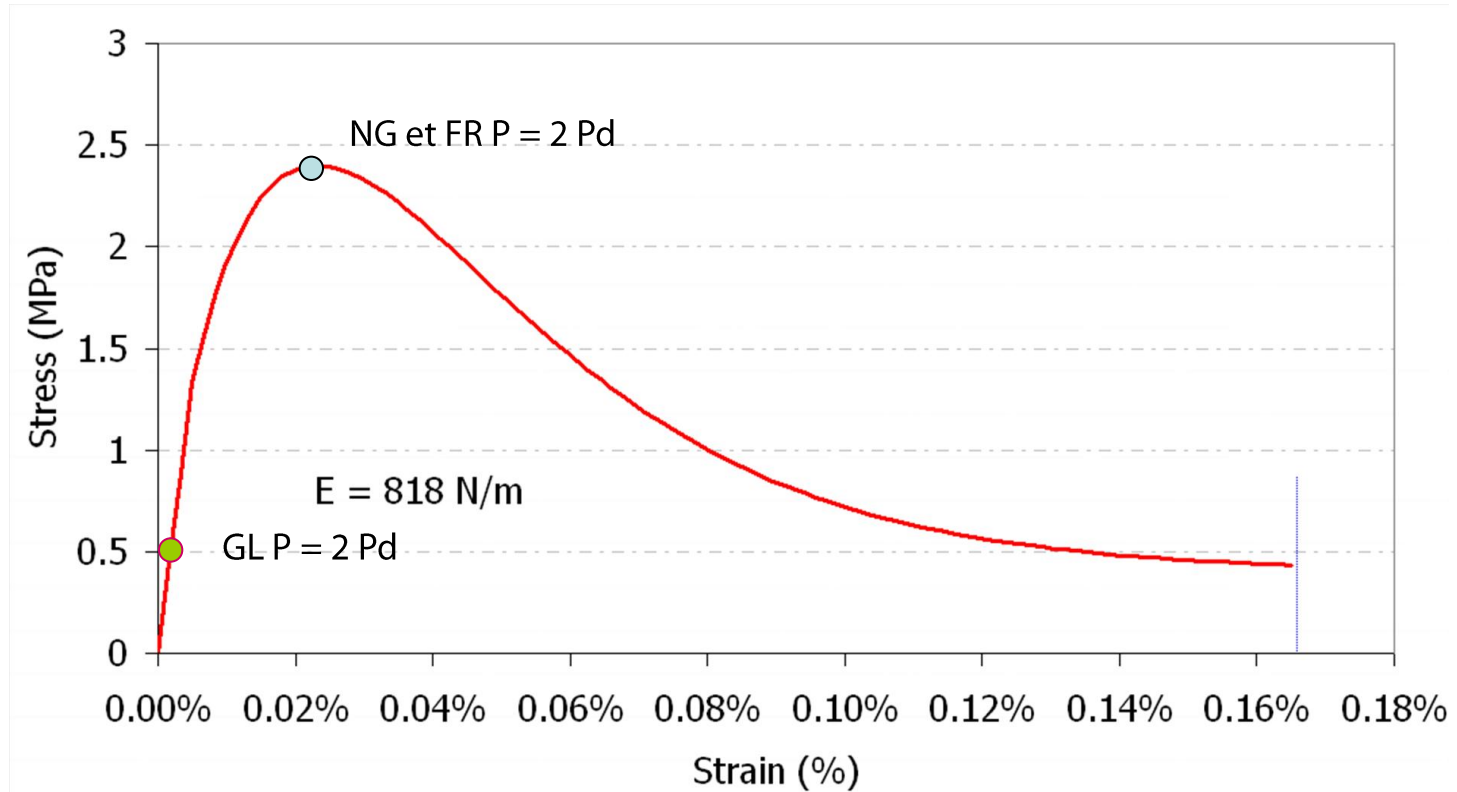
Ungrounded duct



Slippery duct



Sensitivity analyses



Sensitivity analyses: mesh element type

Grouted ducts – Linear elastic analysis

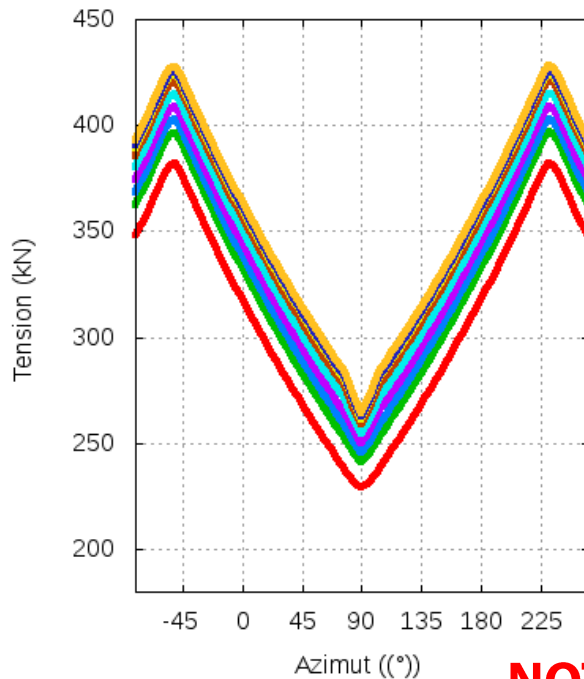
Very slight differences on tendon tensile forces (higher values for linear elements).

Variations are more emphasised with quadratic elements.

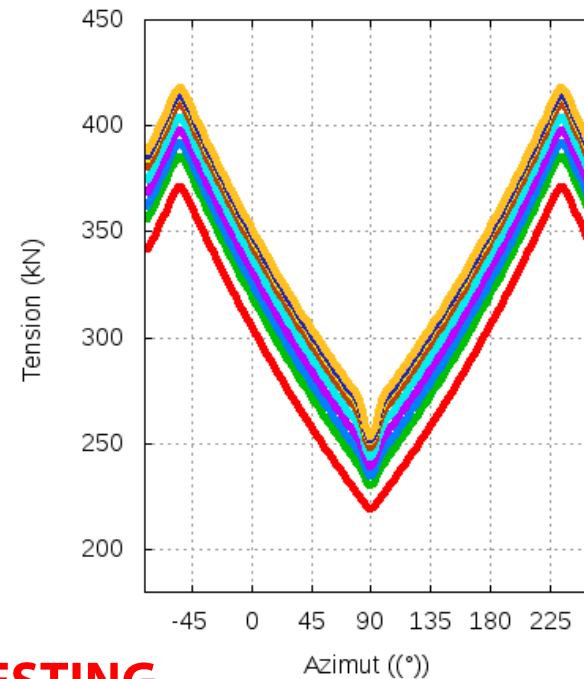
Tendon 67 tension

$P = 0.0 \text{ MPa} (0.0 \text{ Pd})$	— red
$P = 0.4 \text{ MPa} (1.0 \text{ Pd})$	— green
$P = 0.6 \text{ MPa} (1.5 \text{ Pd})$	— blue
$P = 0.8 \text{ MPa} (2.0 \text{ Pd})$	— magenta
$P = 1.0 \text{ MPa} (2.5 \text{ Pd})$	— cyan
$P = 1.2 \text{ MPa} (3.0 \text{ Pd})$	— brown
$P = 1.3 \text{ MPa} (3.3 \text{ Pd})$	— yellow
$P = 1.3 \text{ MPa} (3.4 \text{ Pd})$	— dark blue
$P = 1.4 \text{ MPa} (3.6 \text{ Pd})$	— orange

Coarse linear meshing



Coarse quadratic meshing



NOT VERY INTERESTING

Sensitivity analyses: mesh element type

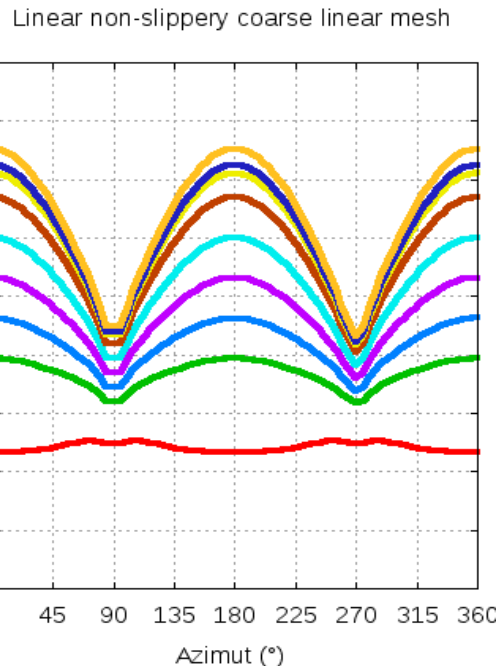
Grouted ducts – Linear elastic analysis

Refined and quadratic meshing produce larger displacement. This is due to the presence of flexural deflection of the model

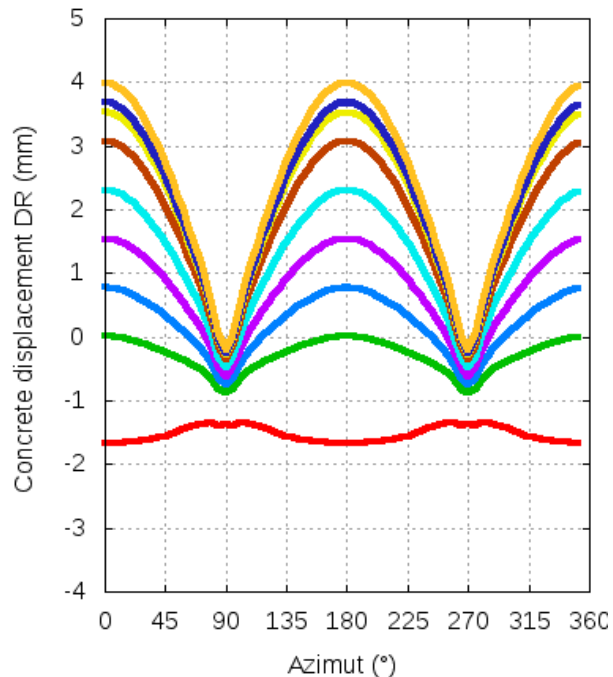
Radial displacement
 $(z = H/2, \text{ external face})$

$P = 0.0 \text{ MPa} (0.0 \text{ Pd})$	
$P = 0.4 \text{ MPa} (1.0 \text{ Pd})$	
$P = 0.6 \text{ MPa} (1.5 \text{ Pd})$	
$P = 0.8 \text{ MPa} (2.0 \text{ Pd})$	
$P = 1.0 \text{ MPa} (2.5 \text{ Pd})$	
$P = 1.2 \text{ MPa} (3.0 \text{ Pd})$	
$P = 1.3 \text{ MPa} (3.3 \text{ Pd})$	
$P = 1.3 \text{ MPa} (3.4 \text{ Pd})$	
$P = 1.4 \text{ MPa} (3.6 \text{ Pd})$	

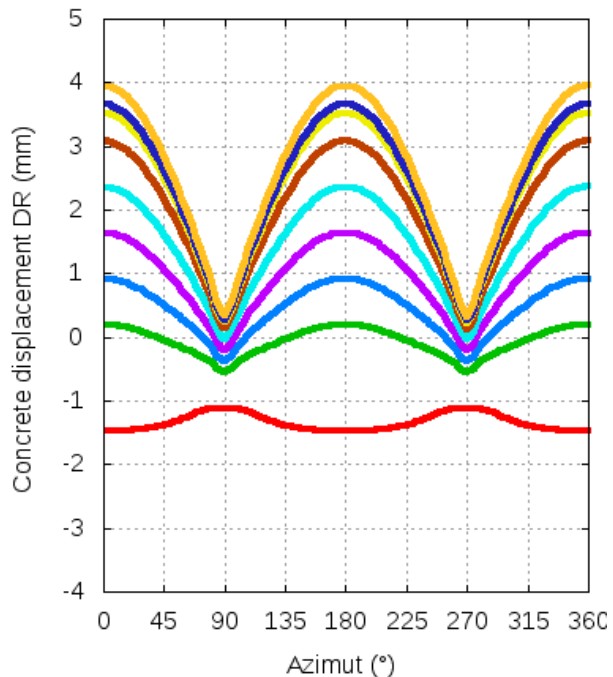
Coarse linear meshing



Coarse quadratic meshing



Refined linear meshing



Sensitivity analyses: mesh element type

Grouted ducts – Linear elastic analysis

Mesh discretisation has a little effect on hoop stress.

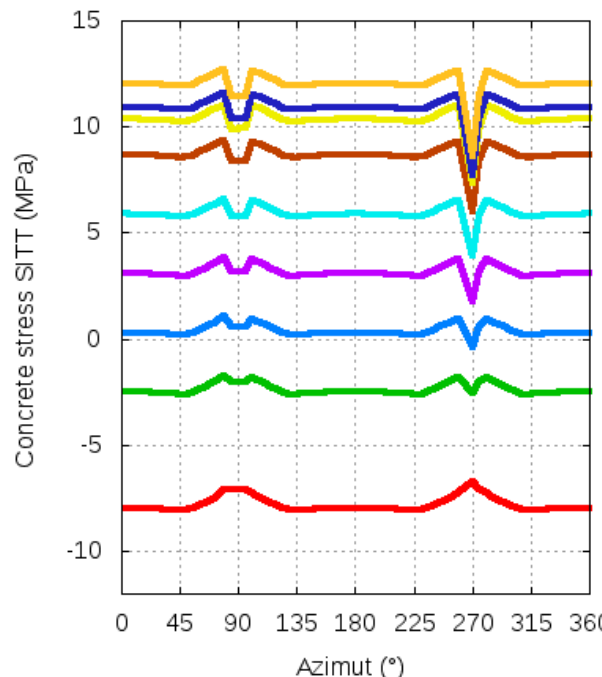
Globally, refined mesh produces lower stresses.

Locally there are slight differences between all cases.

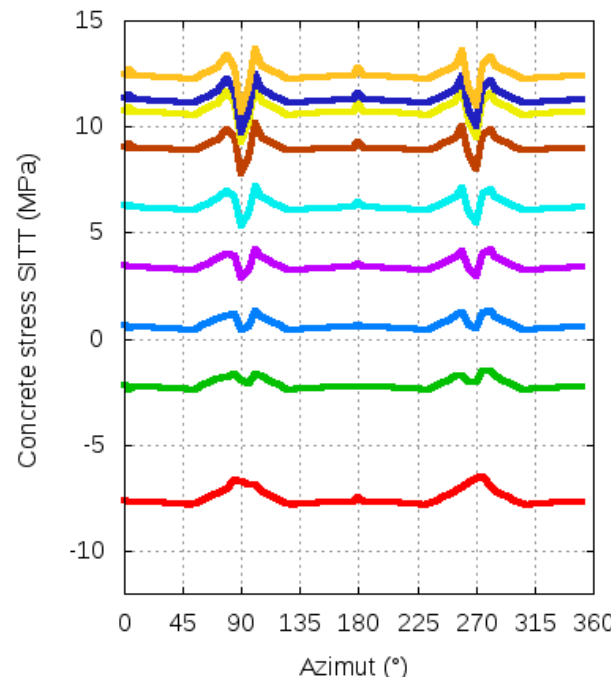
Concrete hoop stress
 $(z = H/2, \text{ mid section})$

$P = 0.0 \text{ MPa} (0.0 \text{ Pd})$	— red
$P = 0.4 \text{ MPa} (1.0 \text{ Pd})$	— green
$P = 0.6 \text{ MPa} (1.5 \text{ Pd})$	— blue
$P = 0.8 \text{ MPa} (2.0 \text{ Pd})$	— magenta
$P = 1.0 \text{ MPa} (2.5 \text{ Pd})$	— cyan
$P = 1.2 \text{ MPa} (3.0 \text{ Pd})$	— brown
$P = 1.3 \text{ MPa} (3.3 \text{ Pd})$	— yellow
$P = 1.3 \text{ MPa} (3.4 \text{ Pd})$	— dark blue
$P = 1.4 \text{ MPa} (3.6 \text{ Pd})$	— orange

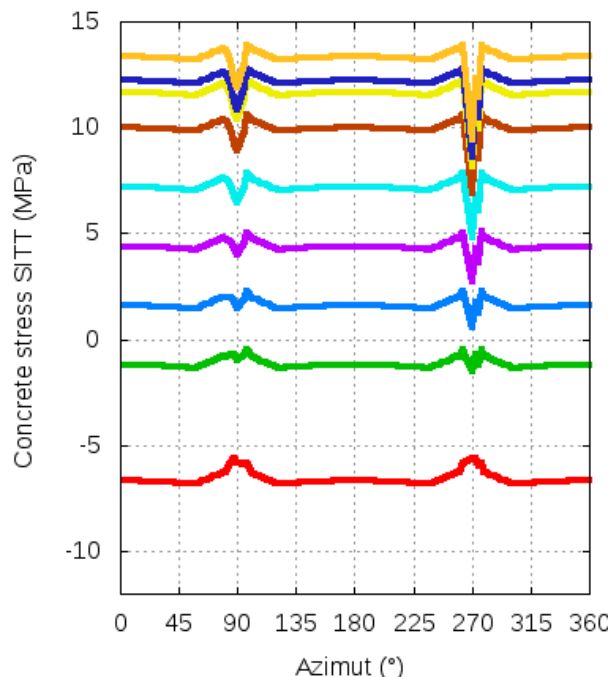
Coarse linear meshing



Coarse quadratic meshing



Refined linear meshing

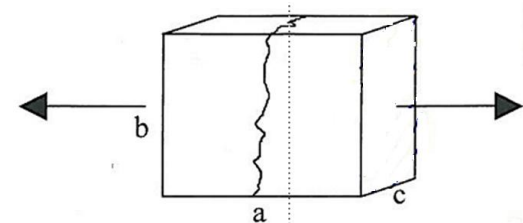


Sensitivity analyses: G_f fracture energy

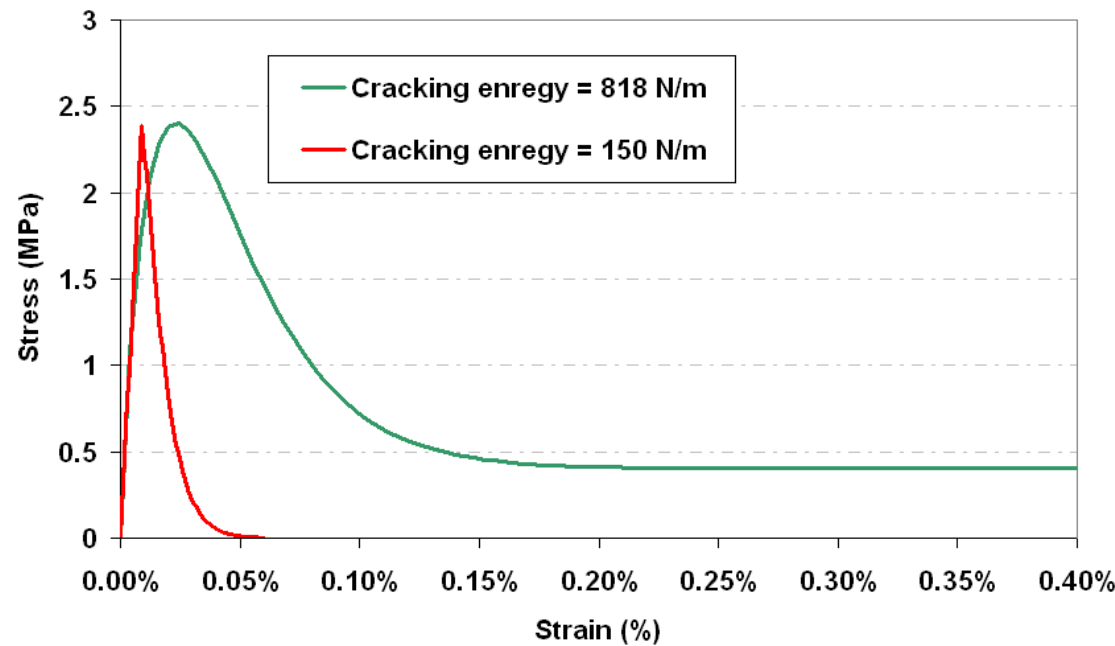
Ungrooved ducts

Cracking energy effect (CEE): Cracking energy. Non-Grouted duct

Energy needed to fracture a concrete bloc = $G_f \times b \times c$



Concrete behavior: Cracking energy 818 N/m vs 150 N/m



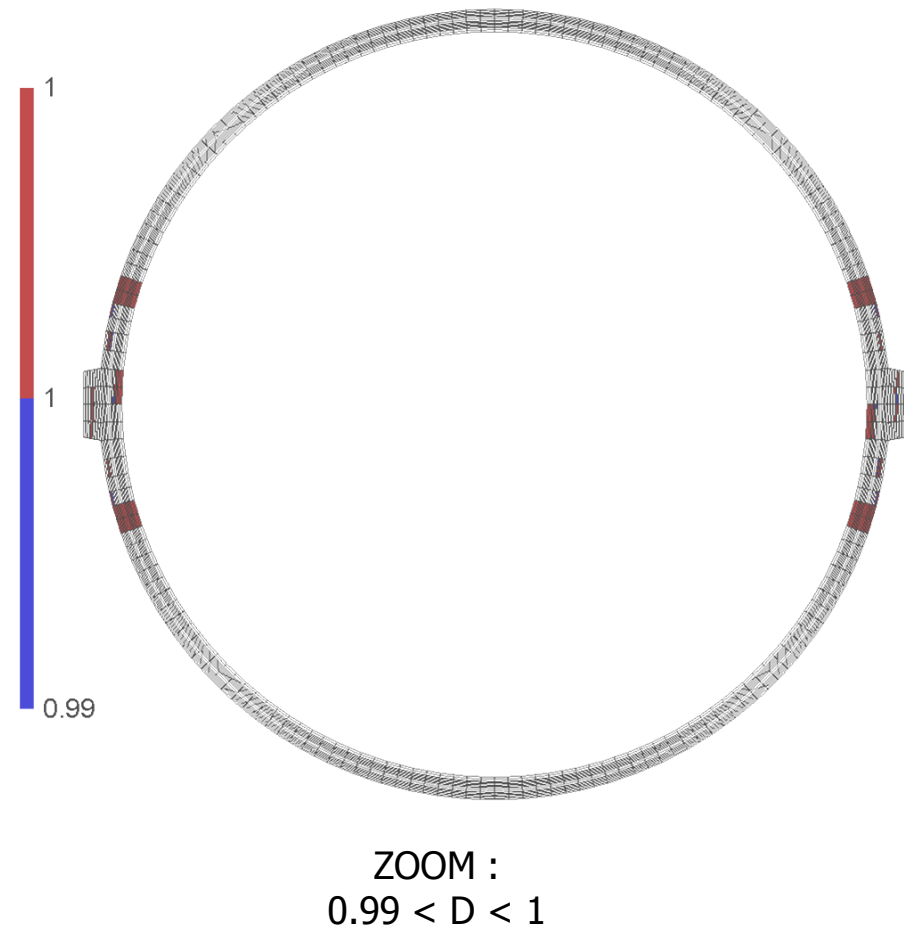
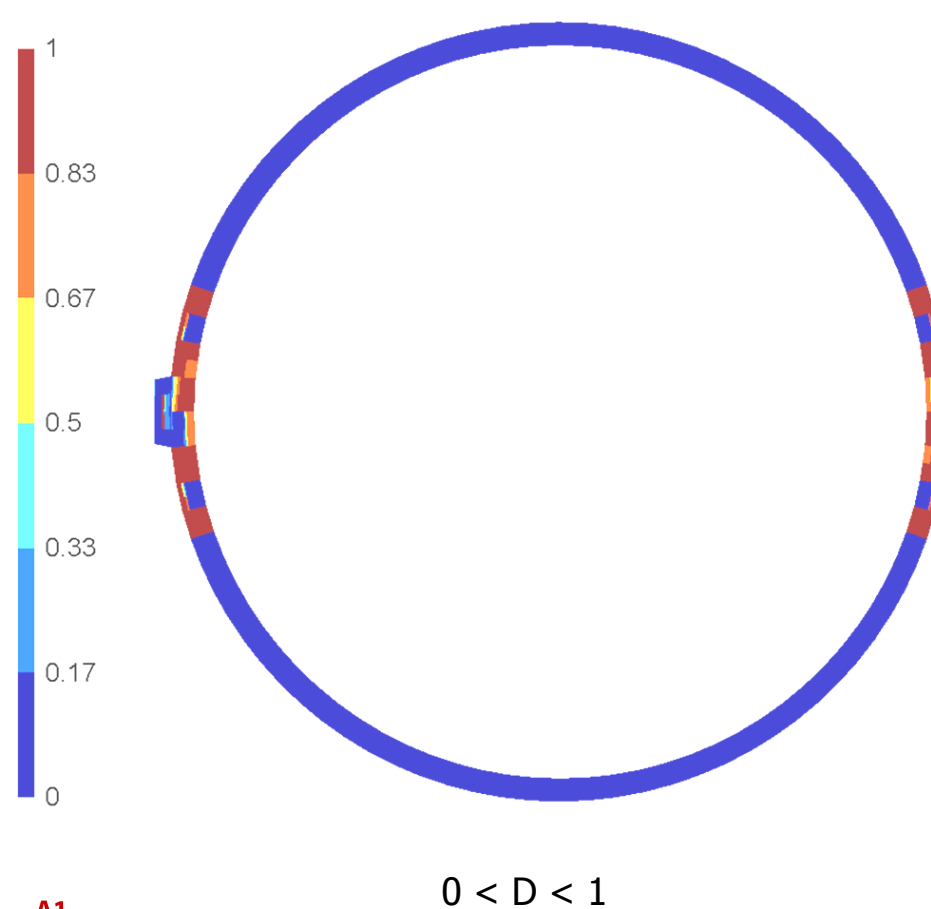
Sensitivity analyses: G_f fracture energy

Ungrouted ducts

Cracking energy effect (CEE): Cracking energy. Non-Grouted duct

Damage index D at $1.7 \times P_d$ ($G_f = 150 \text{ J/m}^2$)

At $P = 1.7 P_d$ full thickness is damaged ($D = 1$) so it can not be loaded any more



Sensitivity analyses: fracture energy effect

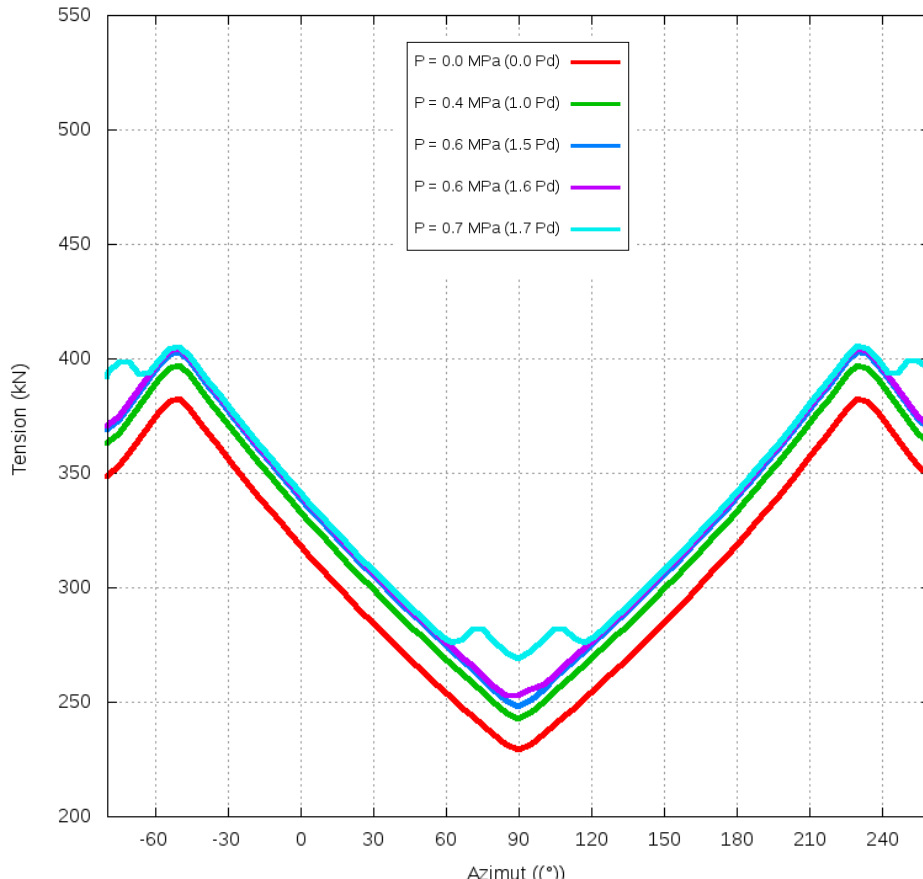
Ungrouted ducts – Nonlinear analysis

Low G_f produces early damaging. Thus early stress concentration in tendons.

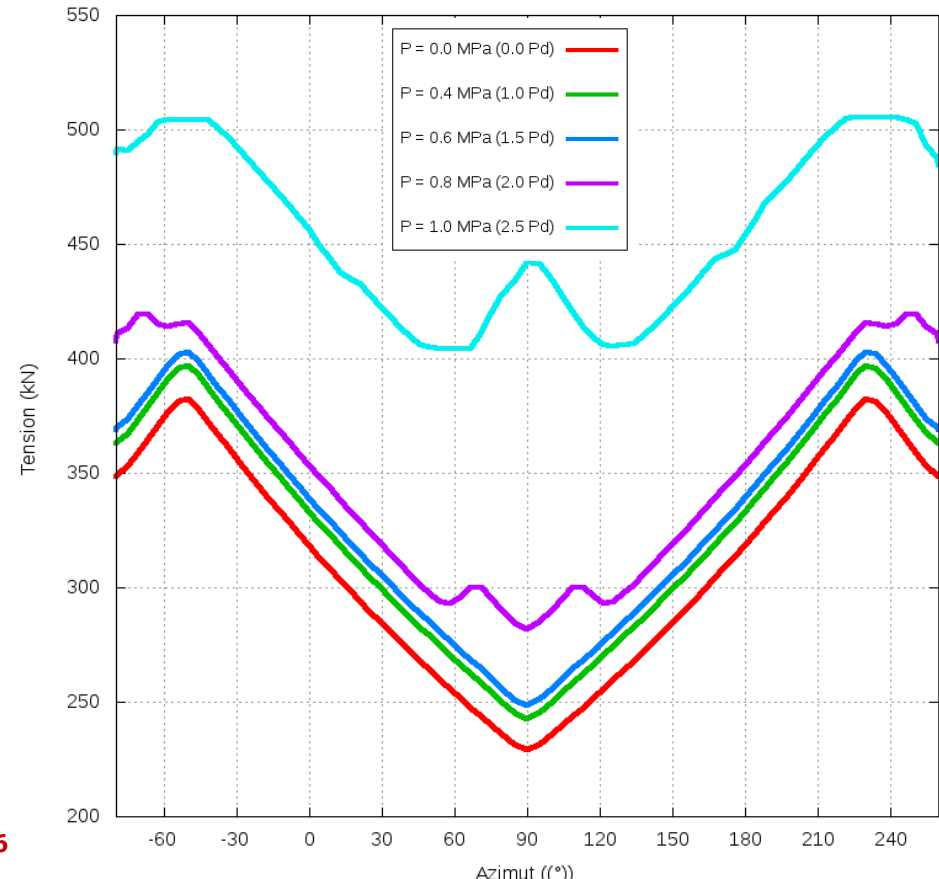
Low G_f raised more difficulties to pursuit calculation (reasons are under investigation). While high G_f allow to reach higher values.

Tendon tension

Concrete M150

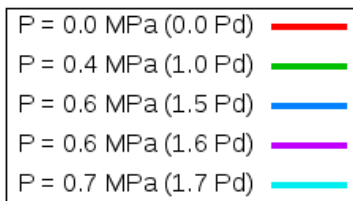


Concrete M818

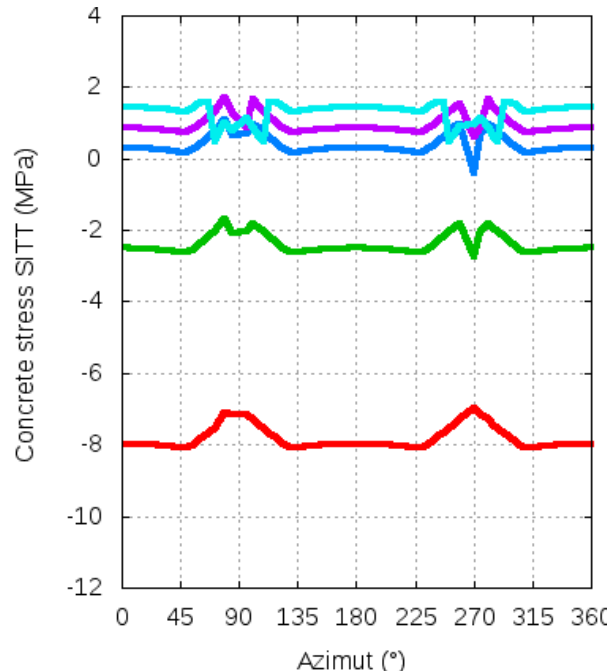


Cracking energy effect (CEE): Concrete hoop stress ($z = H/2$, half thickness). Non-Grouted duct

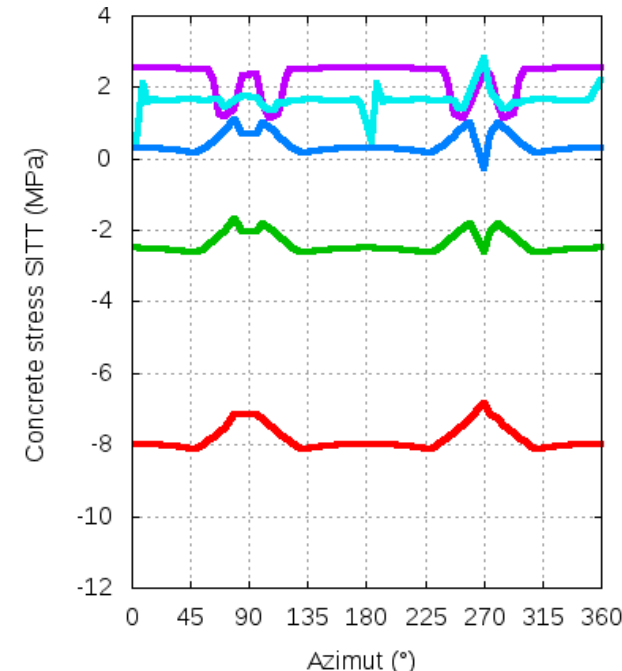
1. Avec l'énergie de fissuration plus basse (150 N/m) à $P = 1.5 \text{ Pd}$ on est proche du pic de contrainte en traction (2.4 MPa) et la partie post-pic de la loi de comportement a une descente brutale ce qui fait que à partir de cette pression l'anneau s'endommage brutalement et le calcul ne converge plus .
2. Avec l'énergie de fissuration plus élevée, à $P = 1.5 \text{ Pd}$ on est loin du pic en traction.
3. Avec l'énergie de fissuration de (150 N/m) on a un comportement plus réaliste mais le fait de n'avoir pas un résidu de résistance au béton complique la convergence du calcul



Non linear (M150) Non-grouted duct



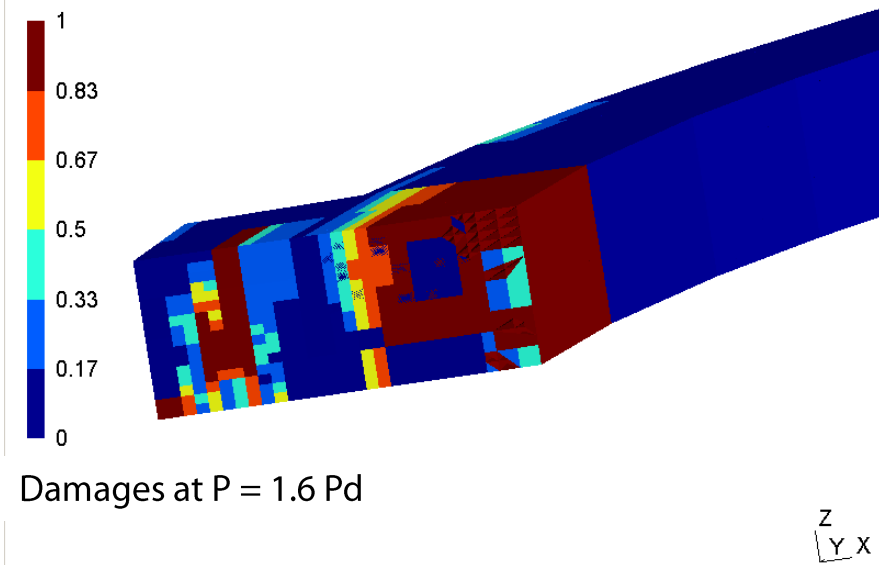
Non linear (M818) Non-grouted duct



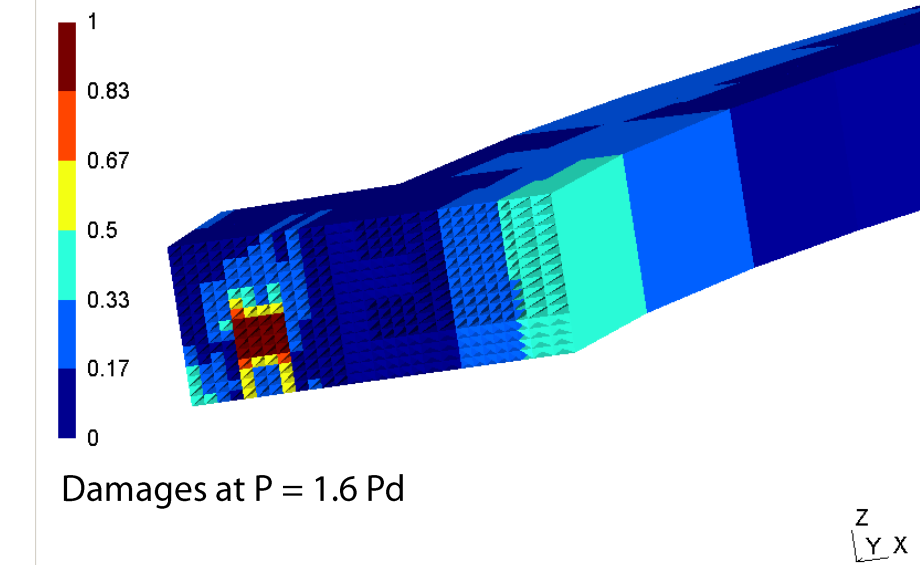
Cracking energy effect (CEE): Concrete damage. Non-Grouted duct

1. Quand l'énergie de fissuration es plus basse (gauche), l'anneau commence à endommager plus tôt (pour la même pression $P = 1.6P_d$ on voit un endommagement plus élevé pour MM150)

Non linear (M150) Non-grouted duct



Non linear (M818) Non-grouted duct

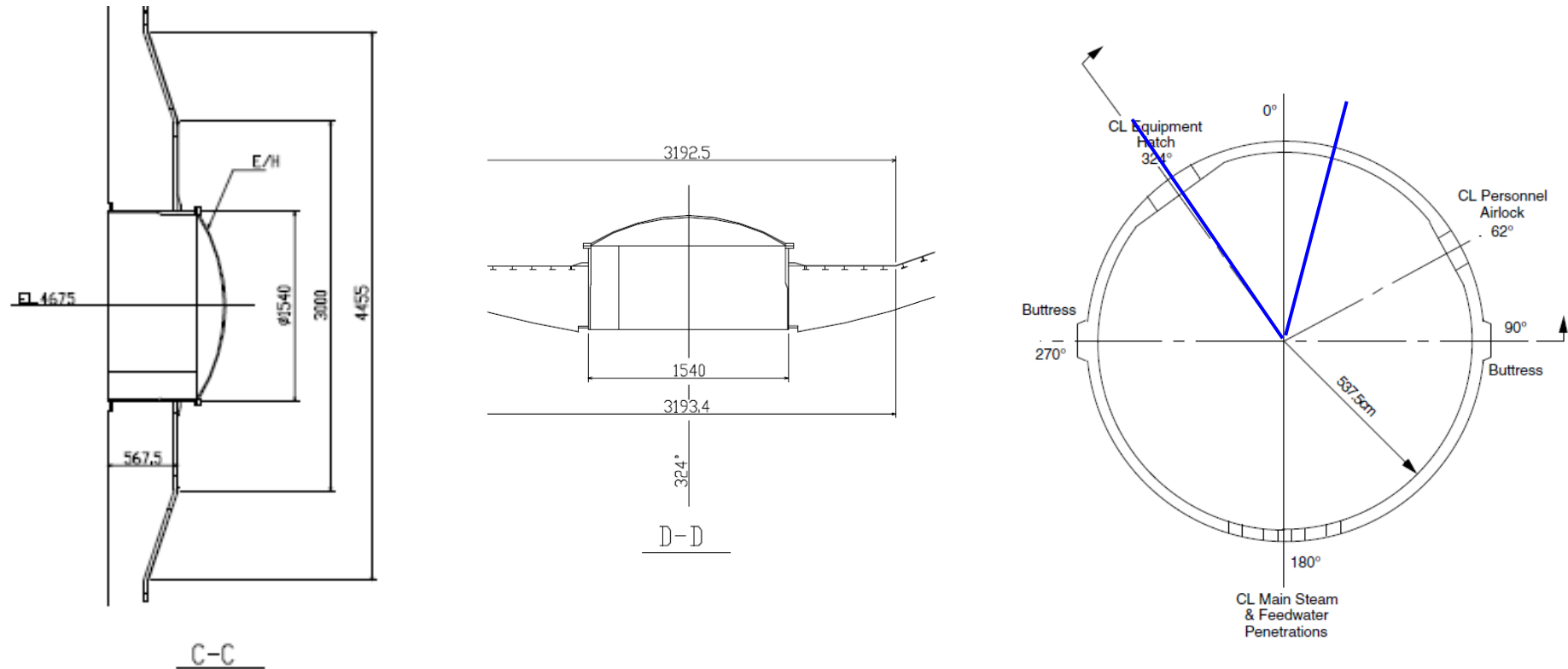


Model 2

SUMMARY

- **Description of equipment hatch geometry**
- **Modeling assumptions and phenomenological models**
- **Description of liner tearing criteria used**
- Deformed shape
- Liner seals state at $p = 0$ (prestress applied), $p = 1.0$ pd

Model geometrical description



From NUREG_CR-6810-appendices.pdf(A-28)

And PCCV-QCON-01

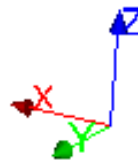
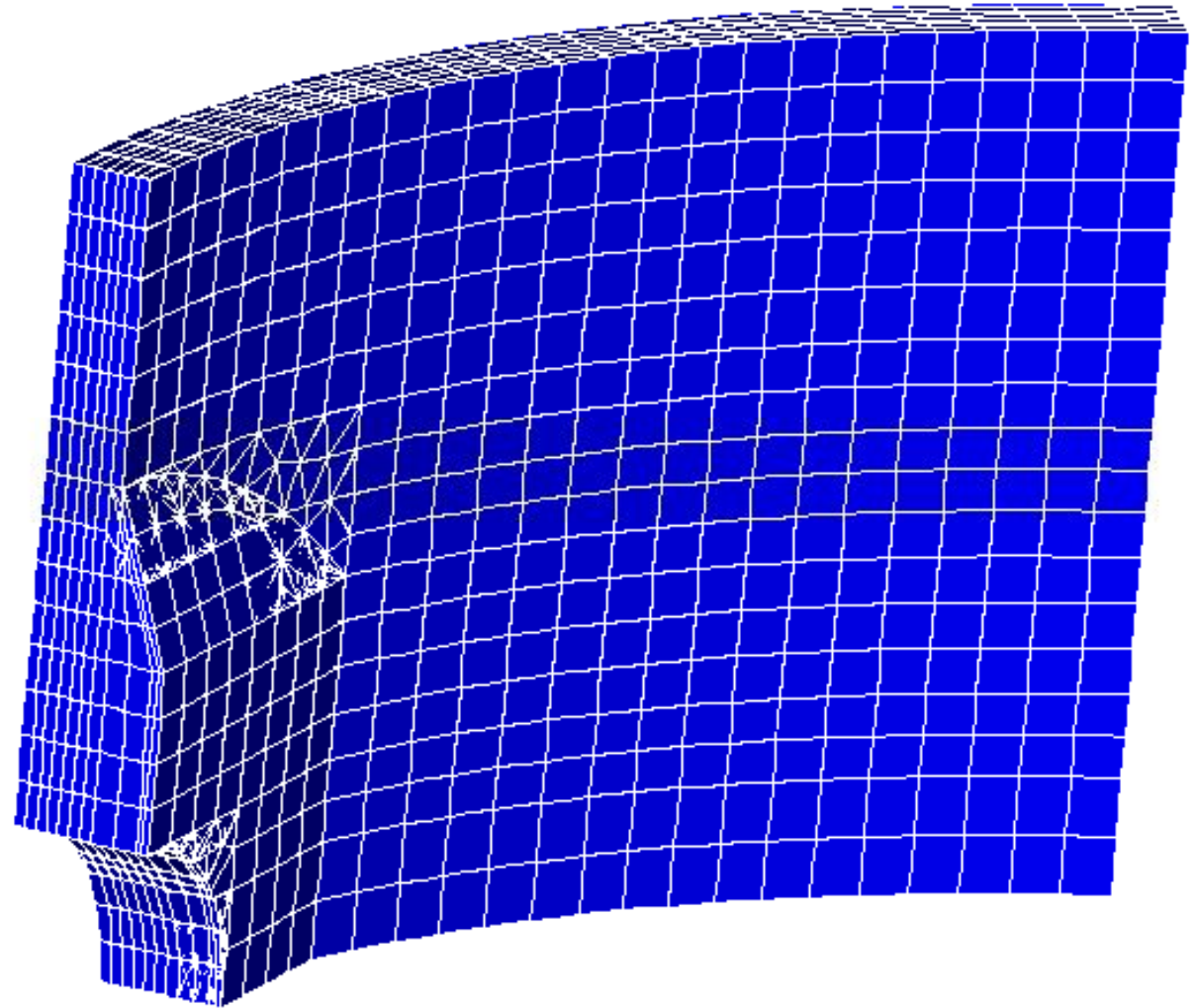
Meshering: concrete

Solid element

Quadratic

Average size = anchorage spacing

Properties: same as for model 1



Meshing: liner

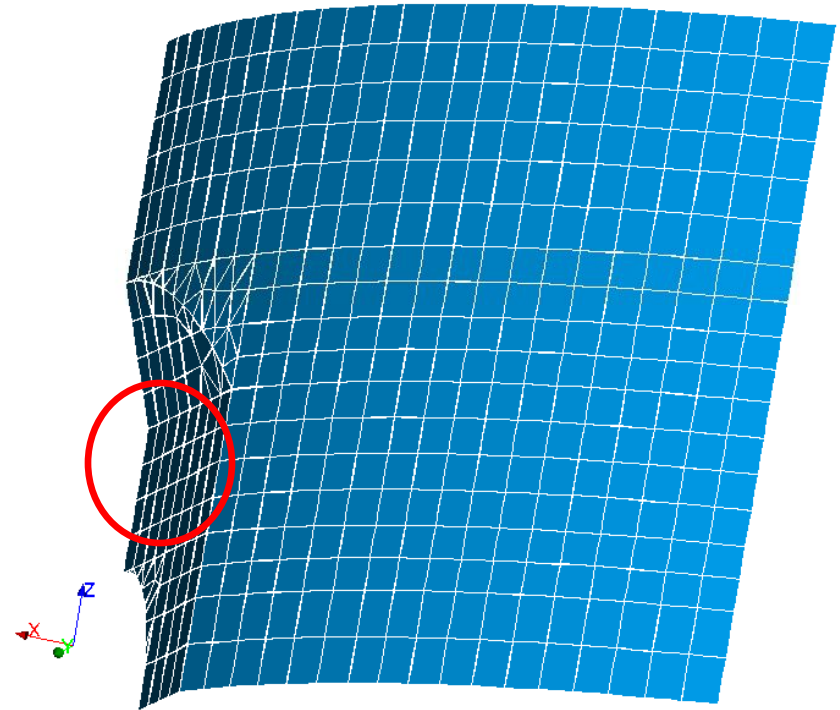
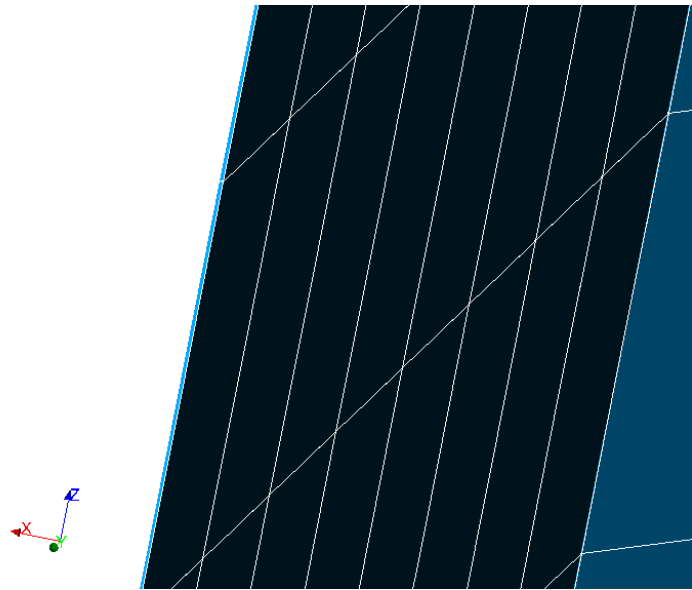
Solid element

Quadratic

Thickness 1.6mm

Liner perfectly bonded with concrete at nodes
except at seal lines (same Ur)

Properties: same as for model 1



Meshering: seal

Cohesive zone model elements

Hexa-CZE (zero volume element)

Quadratic number of nodes with special shape function

Liner / concrete interface: same radial displacement

$E = 223 \text{ GPa}$

$\nu = 0$

$\rho = 7\,850 \text{ kg/m}^3$

$GC = 130 \text{ MPa.}\mu\text{m}$

$SIGM_C = 498 \text{ MPa}$

$COEF_EXTR = 0$

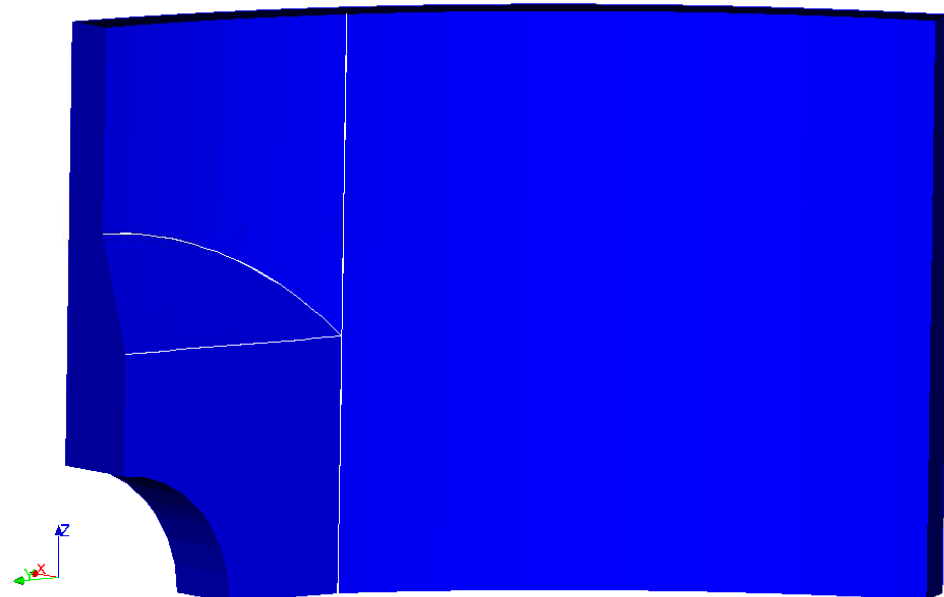
$COEF_PLAS = 0.5$

Surface energy density

Failure stress

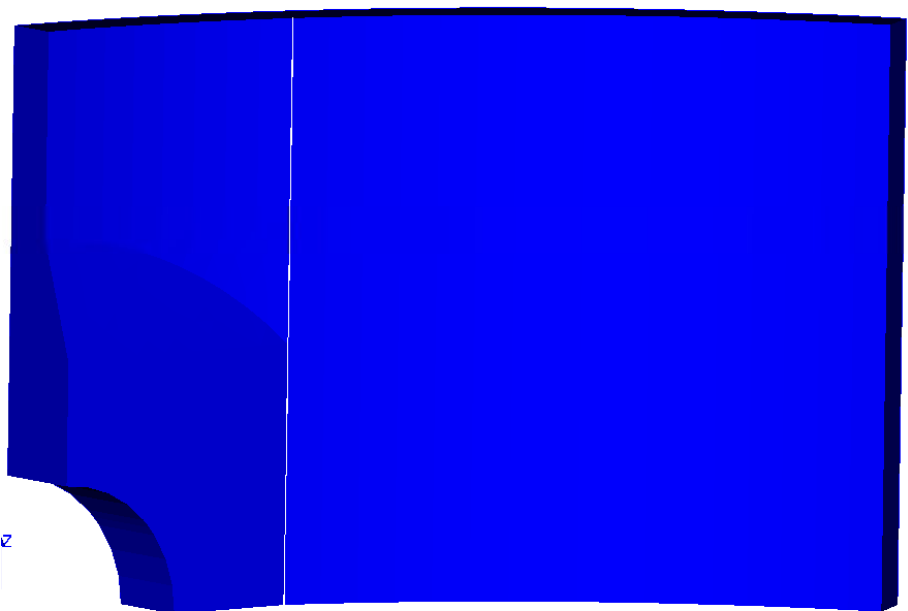
Shape of stress vs jump displacement
curve - Mode I crack opening

Seals surrounding the E/H



A1 Difficulties at intersections!

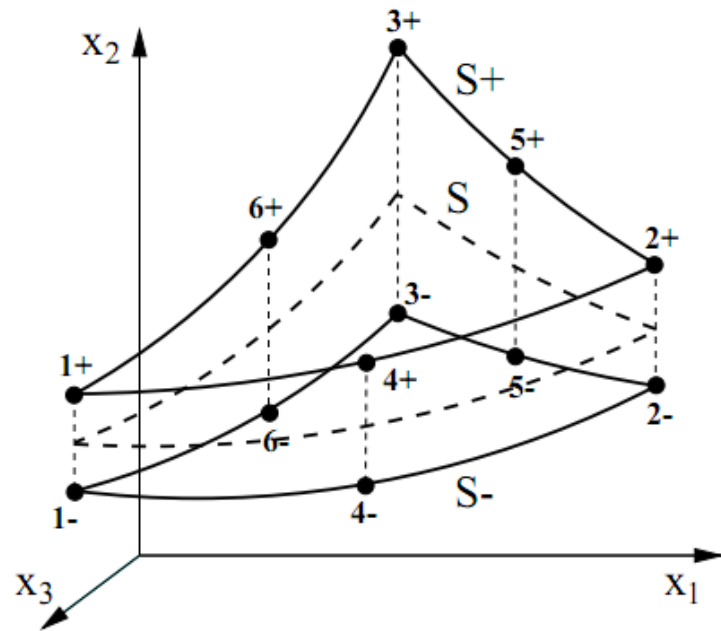
One vertical seal



33

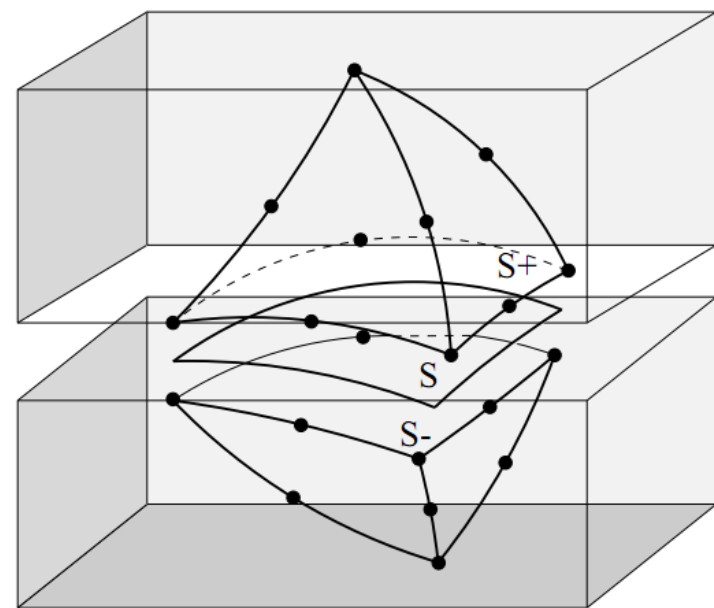
Cohesive zone model elements

Example of tetra-cohesive zone elements. In model 2 we use hexa-CZE.



Geometry of a cohesive element

$S+$ and $S-$ are coincident in initial state



Assembly of a cohesive element with adjacent liner elements

Liner tearing constitutive model

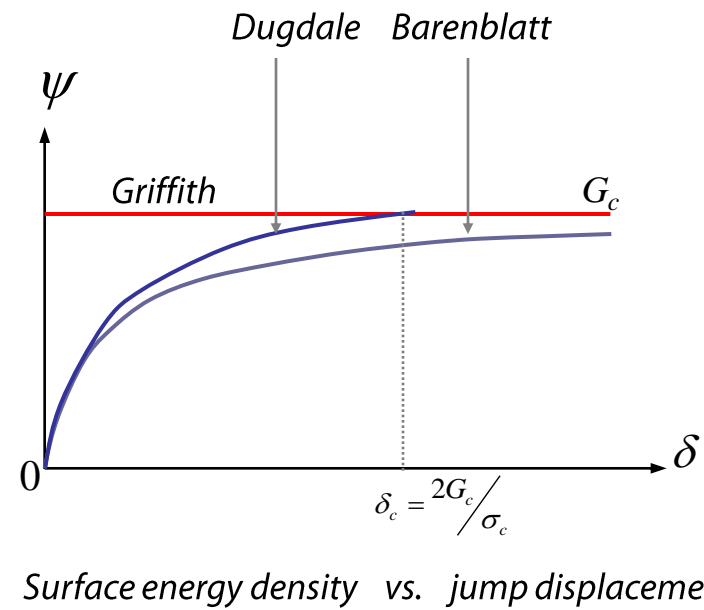
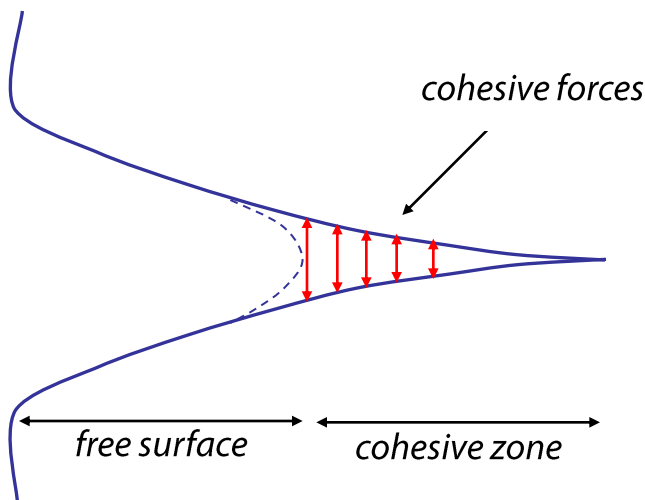
Known as "CZM", Cohesive zone model

Features :

- Energy formulation for failure: minimization of the total energy

$$E_T = \Phi + \Psi - W^{ext}$$

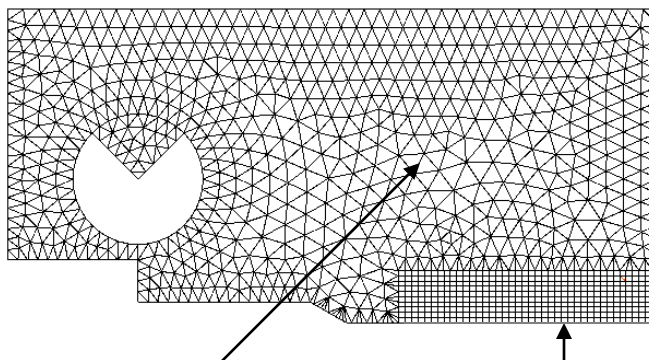
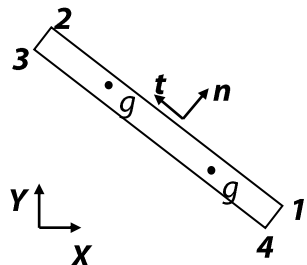
(deformation, external forces, surface)



Liner tearing constitutive model

Known as "CZM", Cohesive zone model

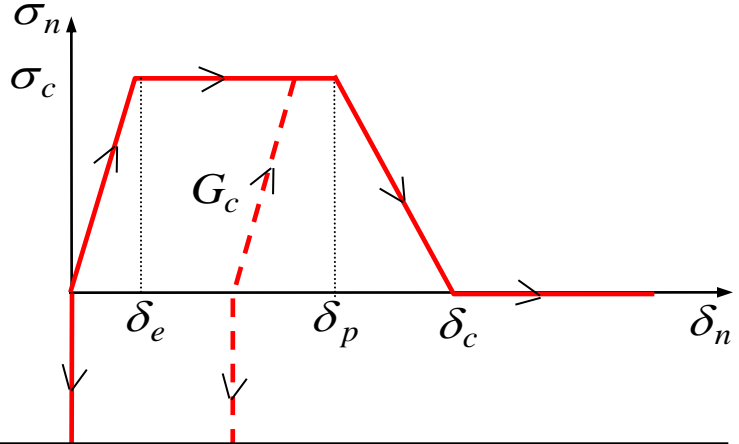
Interface elements introduced along the « supposed » crack path



Sound material
(elastic or elastoplastic)

Interface elements

The cohesive law for ductile fracture



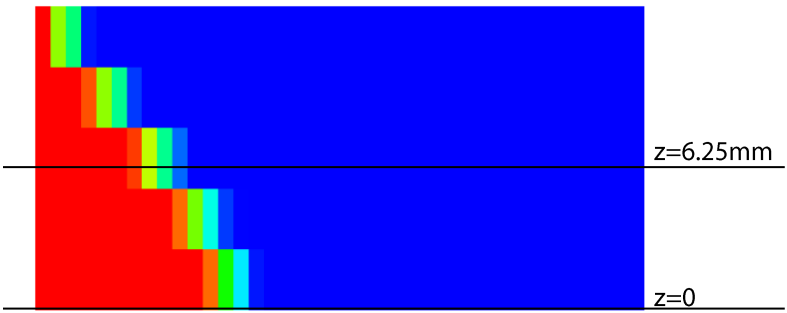
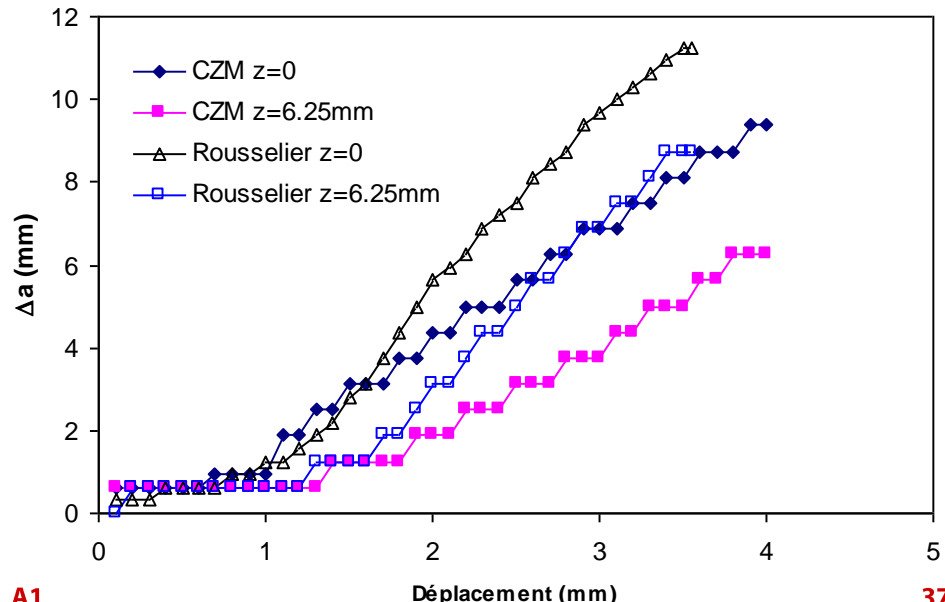
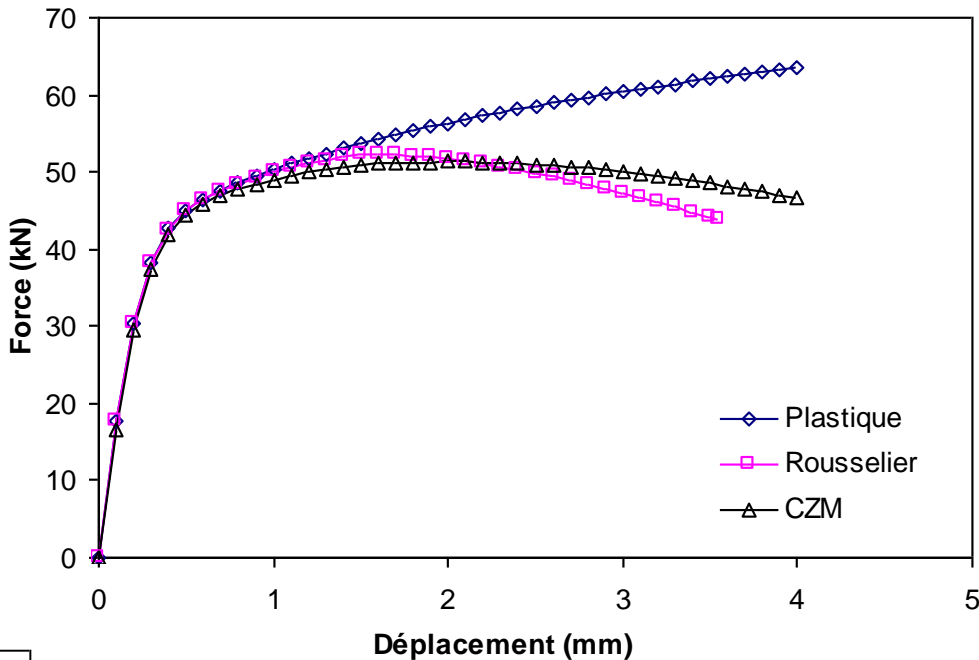
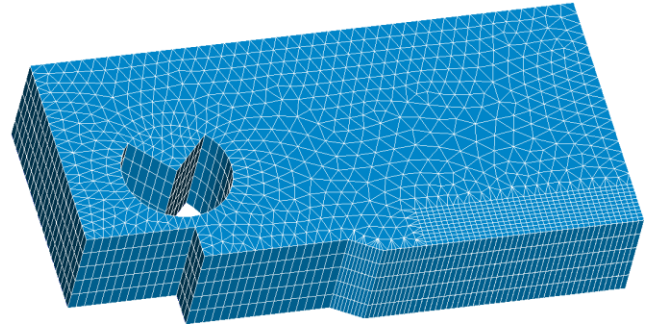
$$\sigma_n(\delta_n) = \sigma_c \begin{cases} \frac{\delta_n}{\delta_e} & \text{if } \delta_n \leq \delta_e \\ 1 & \text{if } \delta_e < \delta_n < \delta_p \\ \frac{\delta_c - \delta_n}{\delta_c - \delta_p} & \text{if } \delta_p \leq \delta_n < \delta_c \\ 0 & \text{if } \delta_n \geq \delta_c \end{cases}$$

$$\delta_c = 2G_c / \sigma_c + \delta_e - \delta_p \quad \delta_e \leq \delta_p < \delta_c$$

Liner tearing constitutive model

Known as "CZM", Cohesive zone model

Test case



Meshering: steel reinforcement

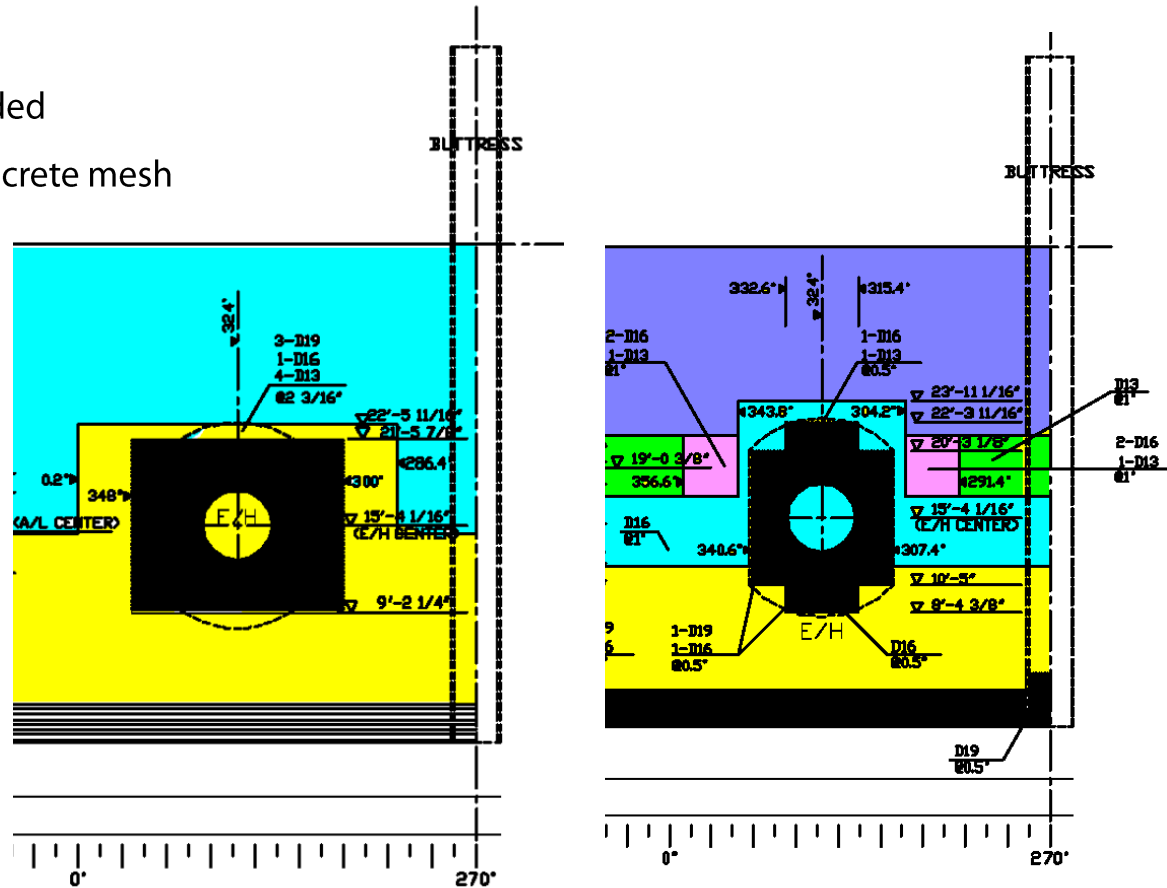
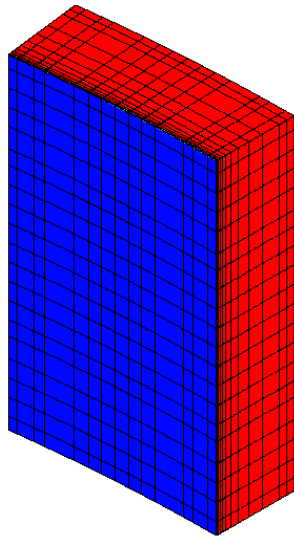
Grid elements

Shell element with uniaxial behaviour

Linear

Rebar / concrete interface: perfectly bonded

Placed on inner and outer surfaces of concrete mesh

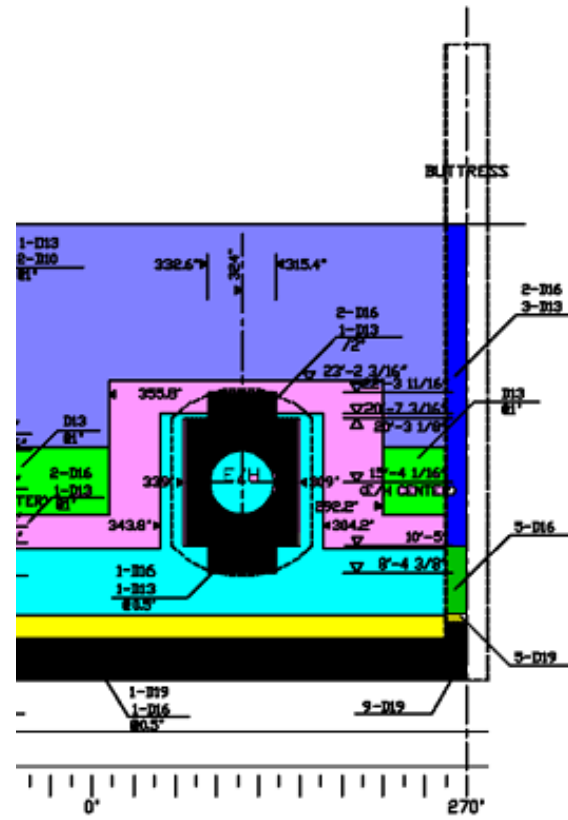
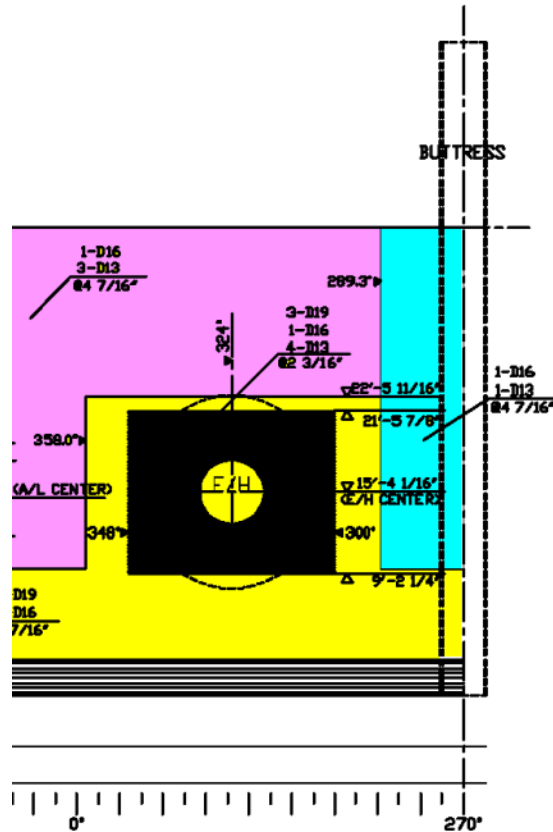


Rebars ratios and localisations (from PCCV-QCON-12 and PCCV-QCON-16)

Inner hoop rebars

Inner vertical rebars

Mesding: steel reinforcement



Rebars ratios and localisations (from PCCV-QCON-12 and PCCV-QCON-16)

Outer hoop rebars

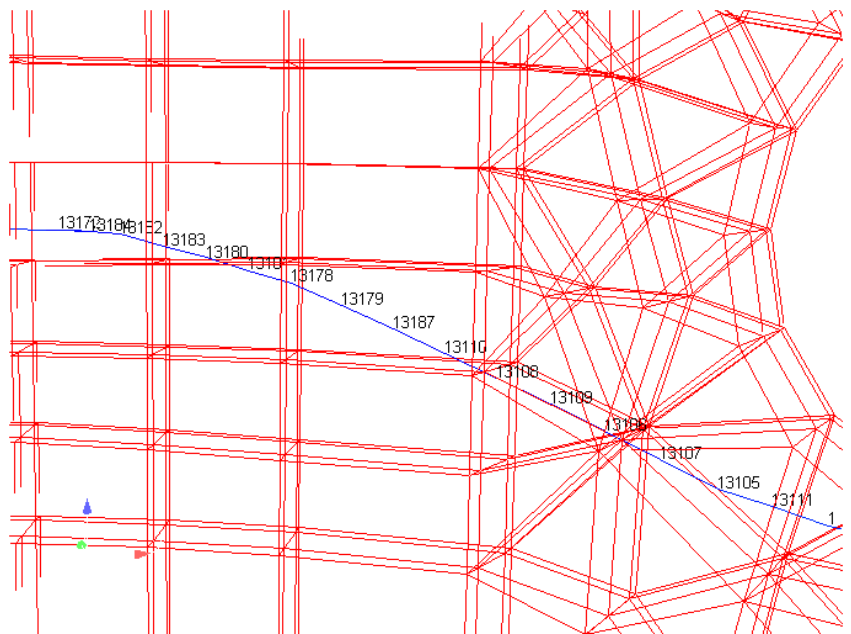
Outer vertical rebars

Meshting: tendons

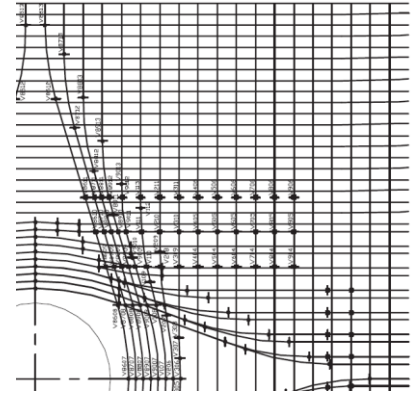
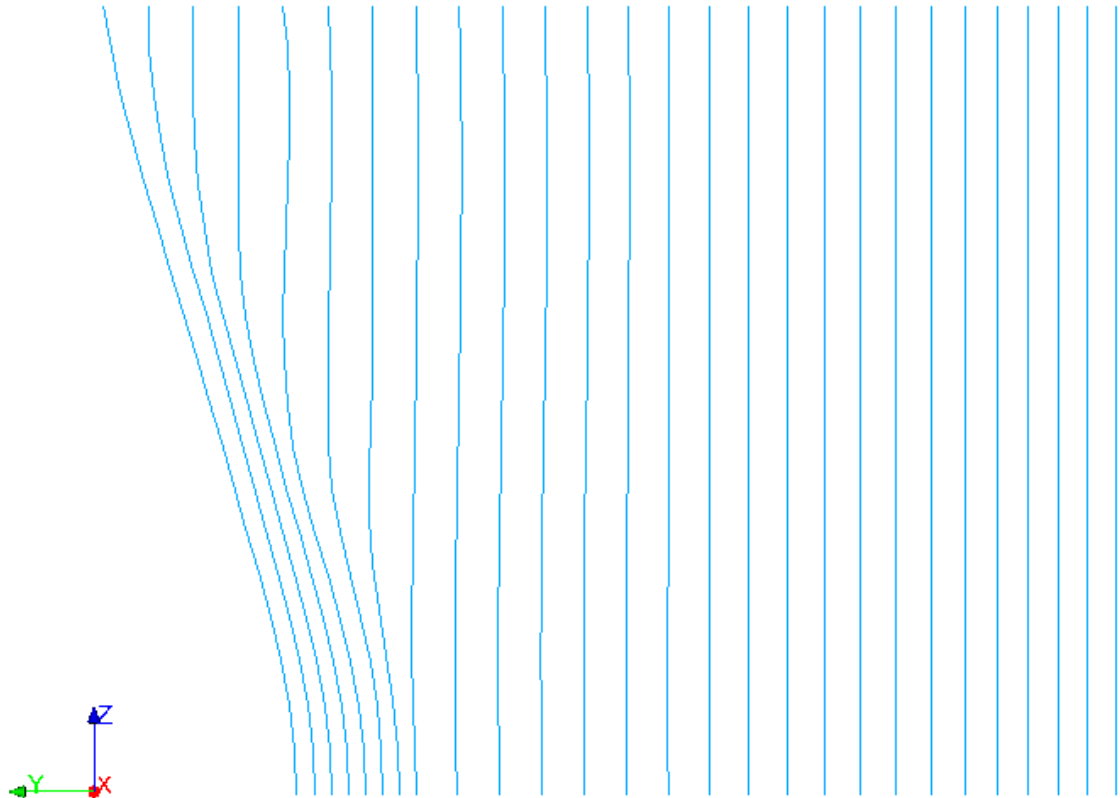
Truss elements

Tendon / concrete interface:

- perfectly bonded in vertical and radial directions
- friction elements between tendon / concrete elements

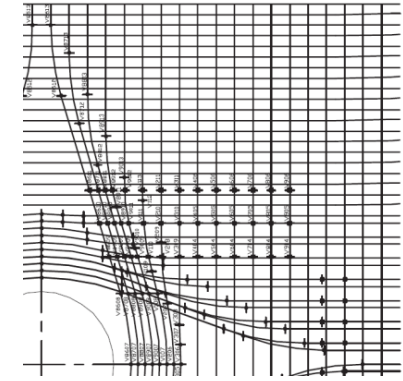
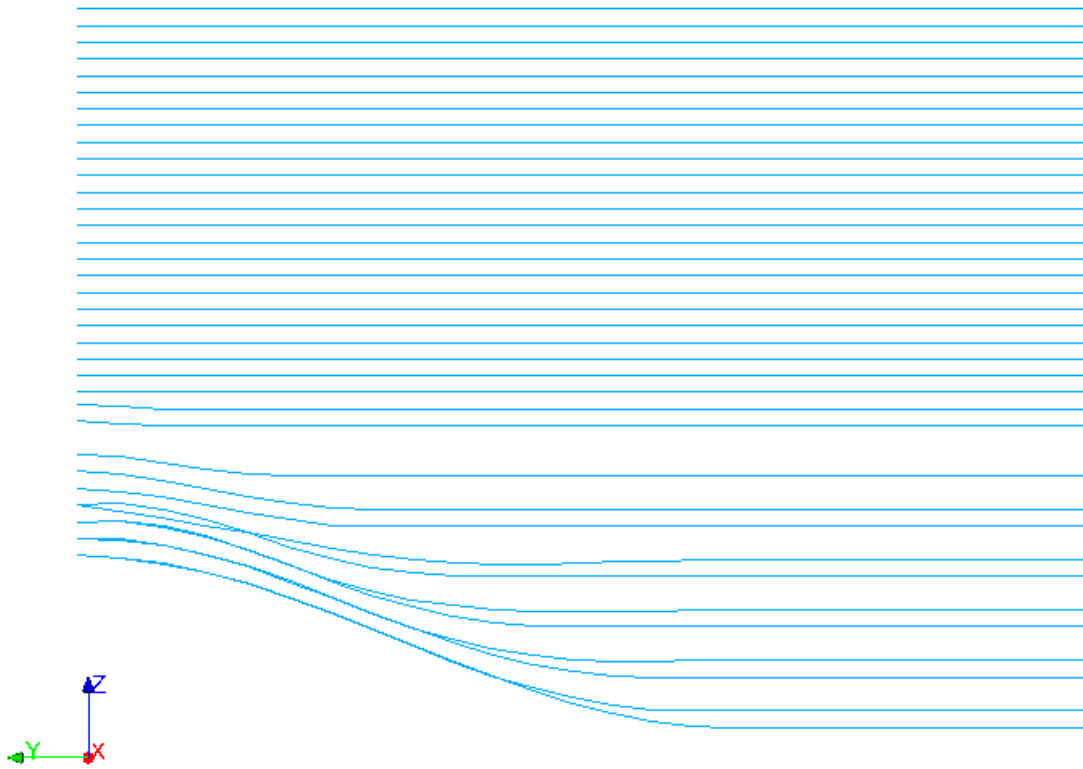


Mesding: tendons



*Actual vertical tendons position and inflections
(from PCCV-QCON-07 and PCCV-QCON-08)*

Mesding: tendons



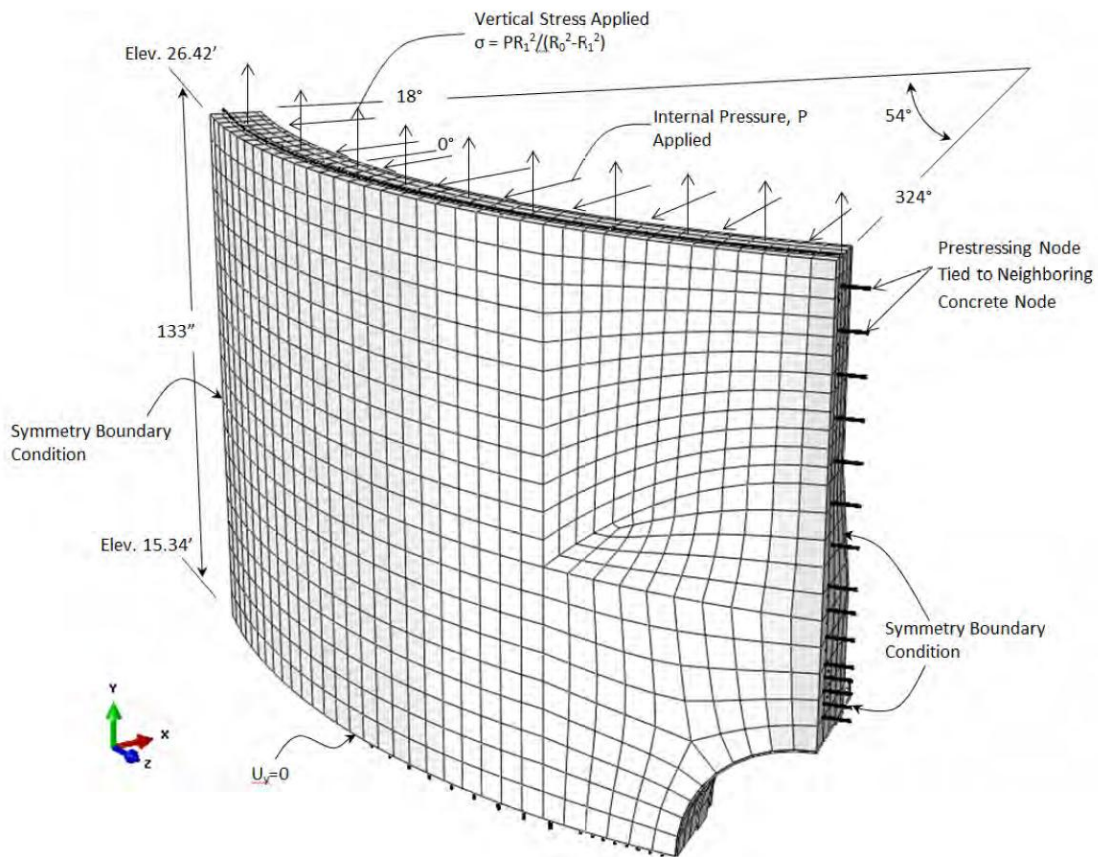
Actual horizontal tendons position and inflections (from PCCV-QCON-07 and PCCV-QCON-08)

Boundary conditions

Lateral surface: rotation constrained to zero

Bottom surface: no vertical displacement

Top surface: vertical stress applied (same as model 1)



Preliminary analyses

Numerical and implementation of CZM elements checks (recently implemented in Code_Aster)

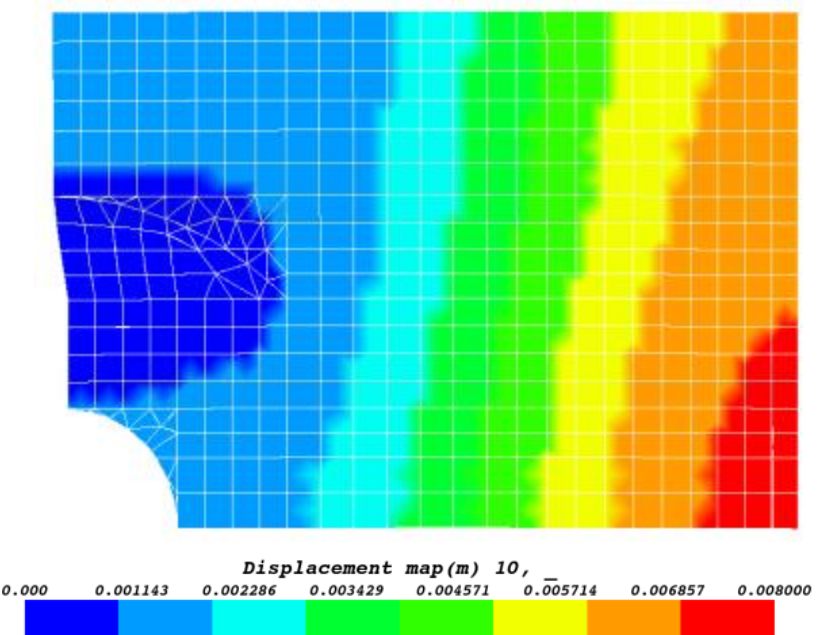
Test analysis 1:

- Concrete remains elastic for tests
- Only one vertical seal
- Prestressing= initial tension set to mean value of tendons A and B close to the E/H
- Increase of internal pressure from 0 up to $3 \times P_d$ in 30 uniform load steps

Test 1: displacement map of liner at $3 \times P_d$ (elastic concrete)

Maximum radial displacement of 7.5mm (half of nonlinear forecasts)

Embossment stiffer than current zone



Preliminary analyses

Test 1: liner tearing within seals (fracture indicator)

Initiation of crack at geometrical and stiffness discontinuity (stress concentration)

Relatively stable calculation

Mesh too refined

Addition numerical implementations needed allowing to simultaneously use both CZM and nonlinear concrete constitutive models

